Polymer Dynamics: A Self-Consistent Field-Theoretic Approach

by

Doug Grzetic

A Thesis

Presented to

The University of Guelph

In partial fulfilment of requirements

for the degree of

Master of Science

in

Physics

Guelph, Ontario, Canada

ABSTRACT

POLYMER DYNAMICS: A SELF-CONSISTENT FIELD-THEORETIC APPROACH

Doug Grzetic
University of Guelph, 2011

Advisor:
Professor Robert Wickham

We develop a self-consistent field theory of polymer dynamics, based on a functional integral approach, which is analogous to the existing equilibrium self-consistent field theory for polymers. We apply a saddle-point approximation to the exact dynamical theory, which generates a set of mean-field equations for the time-dependent density and mean force field. We also develop a method of treating the single-chain dynamics exactly, subject to this mean-field, resulting in a functional Fokker-Planck equation that must be solved along with the mean-field equations in a self-consistent manner. To test the self-consistency, we apply the theory to the simple but non-trivial case of n_P Brownian particles in one dimension interacting via a short-range repulsion in a harmonic external potential. Results for the non-interacting case agree with the literature. The interacting case demonstrates physically sensible interaction-dependent dynamics, such as an increased broadening of the density field when the repulsion is increased. We also examine the dynamics of a binary system with two distinct particle species. We calculate the center-of-mass trajectories for colliding distributions of species A and B, and observe that when the difference of repulsion strengths

between like and unlike species χ is greater than a threshold value (between $\chi = 0.3$ and $\chi = 0.4$), the two species do not mix (indicating the onset of phase segregation).

ACKNOWLEDGEMENTS

I'd like to thank my friends, my girlfriend and my family for their support. I'd also like to thank An-Chang Shi for his input in the early stages of this project, as well as Don Sullivan and Bernie Nickel for being on my supervisory committee. I'd also like to thank Bernie Nickel for his input in the development of Equations 4.36-4.40 regarding the equilibrium solution to the Fokker-Planck equation in the interacting case. Finally, I'd like to thank my supervisor Rob Wickham for his guidance which has been essential, as well as for giving me the opportunity to work on this fascinating project.

Contents

List of Figures

Chapter 1

Introduction

Polymers play an important role in both technology and biology, but their dynamical behaviour is in many cases ill-understood and is a focus of much research. The passage of a protein through a cell membrane, for example, is crucial to biological function and is an interesting problem in polymer dynamics. Polymer translocation, which describes the phenomenon whereby a polymer passes between two regions through a narrow constriction or pore, can be used as a model to study such a biological process. Here one is interested, for example, in the passage time (or *translocation time* τ) and

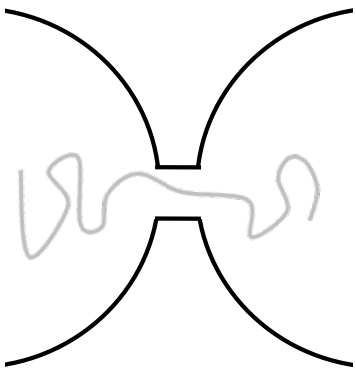

Figure 1.1: A schematic diagram of translocation. The translocating polymer, shown in grey, is in the process of threading the pore.

how it depends on the properties of the system. The translocation time has been shown to depend on parameters such as the chain length and stiffness, properties of the pore such as size and length and properties of the environment such as the driving potential (electrical, chemical, etc.) and crowding effects [2–6]. Qualitatively different translocation regimes are often observed as different regions of the broad parameter space are explored.

Another example of an interesting dynamical problem is electrophoresis, which involves the motion of a polymer under the influence of an electric field, through an array of obstacles such as a gel [7]. If a polydisperse system of polymers passes

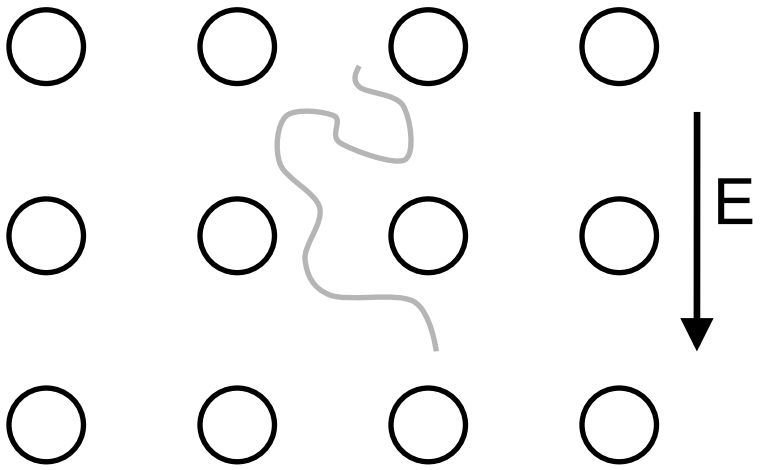

Figure 1.2: A schematic diagram of electrophoresis. The polymer, shown in grey, diffuses through the array of obstacles under the influence of the electric field.

through an array with sufficiently small spacing between obstacles, polymers of higher molecular weight get "hung up" on the obstacles and, in doing so, move more slowly through the array. Gel electrophoresis exploits this behaviour and is used to separate DNA molecules based on their size. A particularly interesting dynamical phenomenon arises when the obstacles become sufficiently dense that the motion of a given polymer is constrained to be primarily along its backbone; this snake-like motion is referred to as reptation. The reptation concept is key to understanding the rheology of polymer melts [1]. The problems just described are closely related and fundamentally they

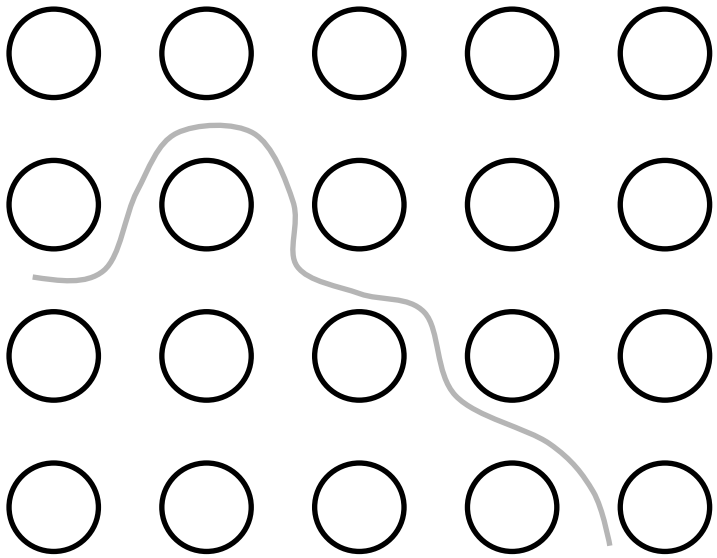

Figure 1.3: A schematic diagram of reptation. The array of obstacles is dense enough that the reptating polymer, shown in grey, is forced to move primarily along its backbone, a result of the topological constraints on the polymer due to the surrounding obstacles.

involve the dynamics of a polymer in the presence of obstacles, which can be modelled as an external potential acting on the chain. A number of experiments, theories and simulations have been employed to study these related problems [7–9], but most theoretical studies to date have involved simulation of particle-based models. What the field of theoretical polymer dynamics lacks is a satisfactory dynamical theory that would play the same role as equilibrium self-consistent field theory (SCFT) does in the equilibrium studies of polymers; that is, one that is able to efficiently sample a broad parameter space. The goal of this thesis is to develop a dynamical self-consistent field theory which we believe will be capable of serving that purpose. The complete formalism of the theory will be presented along with a simple application, which serves to test certain technical aspects of the theory and demonstrate that the theory is capable of making physically sensible predictions to challenging problems.

There are a number of established techniques commonly used to study polymer dynamics computationally; these can be categorized as either particle-based or field-based approaches. Simple models of polymers, such as bead-spring models like the

Rouse model, often capture the universal, long-distance properties of polymers quite accurately and are a starting point for both particle- and field-based theories. In molecular dynamics (MD) simulations, Newtonian/Hamiltonian equations of motion are solved directly for each particle of the system [10]. This is conceptually the most straightforward approach and it is also very faithful to the microscopic details. However, it is a computationally expensive technique and so is difficult to apply to large, dense systems such as polymer melts, or to comprehensive parameter-space studies of dynamical behaviour. The computational load is eased by coarse graining, as in Brownian dynamics (BD) where the equations of motion are made stochastic via systematically coarse-graining out the fast dynamics of the solvent molecules [10]. In this way, the interaction between Brownian particle and solvent is written in terms of dissipative drag force and random fluctuation terms that are related via the fluctuation-dissipation theorem. The coarse-graining procedure essentially trades the microscopic detail of MD for the ability to simulate much longer time-scales. A disadvantage of BD, however, is that it is not Galilean-invariant and thus hydrodynamic effects are not incorporated; this limits its applicability. Hydrodynamics is accounted for in dissipative particle dynamics (DPD), which is a modified form of Brownian dynamics that is Galilean-invariant [10].

Field-based dynamics are approaches where the state of the system is described not by explicit particle positions but by collective, spatially varying field variables such as the density field. Such approaches involve some level of coarse-graining not present in the particle-based models. The field-based methods are suited to studying the dynamics of mesoscopic phenomena such as phase transitions in diblock copolymer melts, when atomic-scale details are either not of interest or not relevant to the mesoscopic/macroscopic dynamics. In these cases, the number of degrees of freedom required for a study using a field-based approach will be significantly less than for the particle-based methods [11]. Present dynamical field-based theories involve the

calculation of a functional free energy for the system. This is supplemented with a dynamical evolution equation in which the thermodynamic driving force for density diffusion is a chemical potential calculated from functional derivatives of the free energy. The time-dependent Ginzburg-Landau (TDGL) equation, for example, is a dynamical evolution equation in which the functional free energy is of the Ohta-Kawasaki form [10]. It is based on Landau theory, which is phenomenological and so has the disadvantage of being difficult to connect with microscopic dynamics; however, TDGL simulations have the advantage that they are much faster than particle-based simulations. There are also a number of methods in the literature that are referred to as dynamic self-consistent field theories [12, 13]. The self-consistent aspect of these theories refers to the use of *equilibrium* self-consistent field theory to calculate a free energy or chemical potential which is then supplemented by a model for dynamics, such as Brownian dynamics [14] or a phenomenological evolution equation [12, 13, 15]. The latter type of theories are similar to dynamic density functional theory (DDFT), first applied to polymer systems by Fraaije in 1993 [16]. In both TDGL and DDFT theories, it is common to treat the connectivity of polymer chains approximately in the choice of kinetic coefficient [17]; this is unrealistic in some cases. More accurate treatments of the kinetic coefficient in DDFT simulations have been made possible [18], and even more sophisticated versions of DDFT have been developed that are able to treat reptation [19]. However, the kinetic coefficient remains problematic because its phenomenological origin makes it difficult to relate simulation time to real time, reducing the predictive power of these theories. The field of theoretical polymer dynamics would benefit from a dynamical field theory that does not have these drawbacks.

Within polymer science, one of the most powerful computational tools developed in the past couple of decades is equilibrium self-consistent field theory. Developed by Helfand [20] in the context of block copolymers, it is a numerically-based analytical

technique whose central approximation is the *mean-field approximation*. This approximation can be explained as follows: a system of interacting polymers is replaced with a system of polymers interacting not each with the others *directly*, but each with a *mean field* that is chosen to represent the *average influence* of the others. In 1994, Matsen and Schick employed a reciprocal-space formulation of equilibrium SCFT that, combined with the computational power of the '90s, made detailed calculations of self-assembled structures (within the mean-field approximation) feasible [21]. Since then, equilibrium self-consistent field theory has been used with great success to study the stability of equilibrium structures in polymeric systems [22, 23], including interesting phenomena such as micro-phase separation in diblock copolymer melts. The ability of self-consistent field theory to generate phase diagrams illustrating regions of stability for experimentally observed, complex structures [24, 25] such as disordered, lamellar, gyroid, hexagonal and cubic phases was a spectacular success.

However, there are limitations of equilibrium self-consistent field theory. As the name indicates, it is an equilibrium theory from which dynamical behaviour is not accessible. At present, the closest dynamical analogue to equilibrium self-consistent field theory is *effective medium theory*, proposed by Edwards and Freed, where the dynamics of a single chain in an effective medium (which contains the effects of the other chains) is calculated self-consistently [1, 26]. Though the analogy with equilibrium self-consistent field theory is not completely satisfactory, effective medium theory is similar in spirit to the theory we develop in this thesis. Our approach is based on a theory for the statistical dynamics of classical systems first developed in 1973 by Martin, Siggia and Rose [27]. A functional integral approach to the Martin-Siggia-Rose (MSR) theory was developed in the late '70s [28, 29] and has been applied to polymer systems by several groups [30–32], including Fredrickson and Helfand in 1990 who derived a field-theoretic approach to multi-chain polymer solution dynamics [30]. They, as well as Vilgis et al. [31], have investigated particular approximations to the field the-

ory (specifically, Gaussian and Hartree approximations) that limit the applicability of their approaches: for example, the Gaussian approximation, employed by Fredrickson, neglects terms higher than quadratic order in the density. It is able to *qualitatively* describe correct dynamical behaviour in the dilute to semi-dilute regimes, but is not adequate in the melt regime where higher order density terms cannot be neglected. In contrast, equilibrium self-consistent field theory (which employs the mean-field approximation) is *most* accurate in the melt regime, where fluctuation effects (and thus deviations from the mean-field thermodynamic behaviour) are smallest [11]. By applying an analogous mean-field approximation to a functional integral formalism of the MSR theory, we may take advantage of the powerful numerical SCFT methods already available, as well as present day computing power, in order to solve the resulting dynamical mean-field equations.

In Chapter 2 we express the Rouse model, modified to include an external field and interactions between monomers, as a dynamical functional integral over collective density fields via the established techniques already mentioned. The result is a formalism for an exact dynamical field theory, for the multi-chain interacting polymer problem, which is flexible and capable of treating a wide variety of dynamical phenomena including, but not limited to, translocation, electrophoresis and reptation. The single-chain dynamics is made explicit in the form of a dynamical partition function for a single chain in a fluctuating force field. The novel results of the thesis begin in Chapter 3 where we develop a method of treating the single-chain dynamics exactly, by relating it to a functional Fokker-Planck equation whose solution is a key quantity called the space-time propagator (the time-dependent single-chain conformation probability distribution functional). We then apply a mean-field approximation to the exact theory. The resulting *dynamical self-consistent field theory* consists of a set of dynamical mean-field equations that must be solved self-consistently along with the functional Fokker-Planck equation corresponding to a single-chain interacting with a

mean force field. The self-consistent aspect of the theory is novel in that we must initially guess the mean force field for both space *and* time. In Chapter 4, in order to establish that this procedure works, we apply the theory to the comparatively simple case of n_P interacting Brownian particles in one dimension, in a harmonic trap. The choice of harmonic trap is motivated by the spring force between beads which we will encounter when we begin to work on the full polymer problem. The particles interact via a short-range repulsion and this introduces a non-trivial element to the problem. We examine a single-species system as well as a binary (two-species) system that exhibits macrophase separation. We are able to calculate a self-consistent solution which shows that the dynamical mean-field approximation produces physically sensible results. Applying the theory to the problems of translocation and electrophoresis, and eventually reptation in polymer melts, is left for future work.

Chapter 2

Theory

2.1 The Rouse model

The Rouse model is the basis for a description of polymer dynamics in solution. It is well-known that the static properties of polymers at long length scales are well described by a bead-spring model [1]; the Rouse model extends this notion to model the dynamics as Brownian motion of the beads.

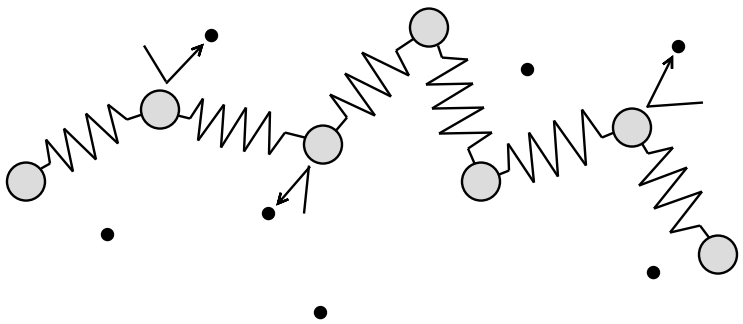

Figure 2.1: The essence of the Rouse model: a bead-spring model of a polymer. Grey spheres represent beads which are shown connected by springs, and black spheres are solvent molecules which buffet the beads.

Note that the beads are not being referred to as *monomers*. This is because monomers of a polymer do not correspond to the beads in the Rouse model. Rather,

the Rouse model is coarse-grained and each bead represents a coiled section of the polymer. In this way the spring force between beads is purely entropic in origin and results from the fact that the entropy of a coiled configuration is higher than the entropy of a stretched configuration. This effect is characterized by the statistical segment length b.

Consider the dynamical evolution of n_P such polymers, each with degree of polymerization N. At time t, the n^{th} bead on the l^{th} polymer has a position $\vec{R}_n^{(l)}(t)$. Different beads interact with one another via a pair-wise interaction force $\vec{F}_{int}(\vec{R}_n^{(l)}(t), \vec{R}_m^{(l')}(t))$ and are subject to an external force field, $\vec{F}_{ext}(\vec{R}_n^{(l)}(t))$. The random thermal force of the solvent buffeting the n^{th} bead on the l^{th} polymer is denoted $\vec{f}_n^{(l)}(t)$ and the spring force between adjacent beads is denoted $\vec{F}_n^{(l)}(t)$. The bead positions $\vec{R}_n^{(l)}(t)$ evolve according to the Langevin equation of motion, which takes the form

$$\begin{aligned} \zeta_0 \frac{\partial \vec{R}_n^{(l)}(t)}{\partial t} &= \vec{F}_n^{(l)}(t) + \vec{F}_{ext}(\vec{R}_n^{(l)}(t)) \\ &+ \sum_{l'} \sum_{m} \vec{F}_{int}(\vec{R}_n^{(l)}(t), \vec{R}_m^{(l')}(t)) + \vec{f}_n^{(l)}(t). \end{aligned} \tag{2.1}$$

Here, ζ_0 is a friction coefficient for the beads. We make the standard assumption that the inertia of the polymer is not important on the time scales of interest; that is, the motion is in the viscous regime. Although the *standard* Rouse model ignores the excluded volume interaction and, more generally, does not include either $\vec{F}_{ext}$ or $\vec{F}_{int}$, we include both $\vec{F}_{ext}$ and $\vec{F}_{int}$ in our treatment. They will remain unspecified for now, but will eventually be chosen to model the specific system of interest. The external force may be chosen to model the external environment (for example, an applied electric field or a periodic array of obstacles), and the interaction force can be chosen to model, for example, polyelectrolytes by choosing a short-range screened Coulomb interaction force, or a polymer melt with the excluded volume interaction by choosing a hard-core repulsive interaction force.

The Rouse model also ignores the hydrodynamic interaction. For concentrated solutions and melts, where the hydrodynamic interactions are screened out, the Rouse model provides a good starting point to describe the dynamics of polymers. It also provides a conceptual framework to study the dynamics of polymers in dilute solution; however, it is incorrect in some details since it does not account for the hydrodynamic interaction. The Zimm model [1] is an improvement on the Rouse model for dilute solutions which incorporates hydrodynamic effects.

For beads that are not at the ends of the chain, $1 < n < N$, the spring force $\vec{F}_n^{(l)}(t)$ acting on the n^{th} bead on the l^{th} polymer at time t has the form

$$\vec{F}_n^{(l)}(t) = \frac{3k_BT}{b^2}\left[\vec{R}_{n+1}^{(l)}(t) - 2\vec{R}_n^{(l)}(t) + \vec{R}_{n-1}^{(l)}(t)\right], \tag{2.2}$$

while for the chain-end beads,

$$\vec{F}_1^{(l)}(t) = \frac{3k_BT}{b^2}\left[\vec{R}_2^{(l)}(t) - \vec{R}_1^{(l)}(t)\right] \tag{2.3}$$

$$\vec{F}_N^{(l)}(t) = \frac{3k_BT}{b^2}\left[\vec{R}_{N-1}^{(l)}(t) - \vec{R}_N^{(l)}(t)\right]. \tag{2.4}$$

The random thermal force is Gaussian-distributed with zero mean

$$\left\langle f_{\alpha,n}^{(l)}(t)\right\rangle = 0. \tag{2.5}$$

It is related to the viscous drag force $\zeta_0\frac{\partial\vec{R}_n^{(l)}(t)}{\partial t}$ by the fact that their physical origin is the same (the action of the solvent particles on the beads). This relationship is expressed by the *fluctuation-dissipation theorem*, which establishes a connection between the magnitude of the correlations between fluctuations (random force) and the friction coefficient (drag force):

$$\left\langle f_{\alpha,n}^{(l)}(t) f_{\beta,m}^{(l')}(t')\right\rangle = 2\zeta_0 k_BT\delta_{\alpha\beta}\delta_{ll'}\delta_{nm}\delta(t-t'). \tag{2.6}$$

The fluctuation-dissipation theorem also serves to maintain the system at a given temperature T [10] and thus ensures that the system is able to relax to thermodynamic equilibrium at late times. In the absence of $\vec{F}_{ext}$ and $\vec{F}_{int}$, the Rouse model can be solved using normal coordinates to decompose the motion of the polymer into independent modes referred to as *Rouse modes*. The Rouse modes evolve independently of one another and averages can be calculated easily. The interacting case, however, is not so simple. To treat the dynamics in this case we resort to a functional integral approach to the Martin-Siggia-Rose (MSR) theory for the statistical dynamics of classical systems [27], developed in the late '70s by De Dominicis and Janssen [28, 29] and later applied to polymer systems by Fredrickson and Helfand [30]. The original MSR theory can be described as a Heisenberg operator theory that parallels the Schwinger formalism of quantum field theory; in this sense, the functional integral approach is analogous to Feynman's path integral formalism of quantum field theory.

2.2 The functional integral

At the initial time t_0, the probability distribution of a particular conformation $\{\vec{R}_n^{(l)}(t_0)\}$ of the l^{th} polymer is given by the probability distribution functional $P_0(\{\vec{R}_n^{(l)}(t_0)\}, t_0)$. We assume that the initial conformations of each of the n_P polymers satisfy the same probability distribution $P_0(\{\vec{R}_n^{(l)}(t_0)\}, t_0)$. We now construct a functional integral $Z_f(t|t_0)$ that sums over all space-time polymer conformations:

$$\begin{aligned} Z_f(t|t_0) &= \int \prod_l \left(\prod_n \{d\vec{R}_n^{(l)}(t_0)\} P_0 \left(\{\vec{R}_n^{(l)}(t_0)\}, t_0 \right) \right) \times \\ &\quad \int \prod_{l,n} \left\{ D\left[\vec{R}_n^{(l)}(t')\right] \delta\left[\vec{R}_n^{(l)}(t') - \bar{\vec{R}}_n^{(l)}(t')\right] \right\}, \end{aligned} \tag{2.7}$$

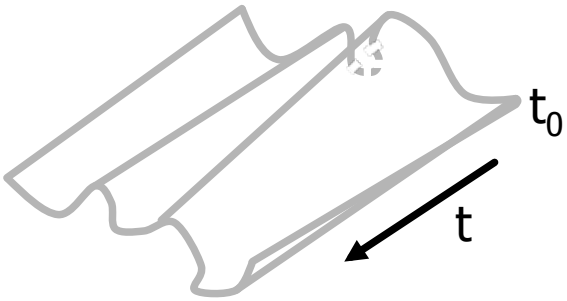

Figure 2.2: Space-time polymer conformations. The trajectory of a particular polymer, starting from the initial configuration $\{\vec{R}_n^{(l)}(t_0)\}$, can be thought of as tracing out a *world-sheet* such as the one shown here. In the functional integral, we sum over *all* such trajectories that satisfy the Langevin equation.

where the functional integral notation is defined by

$$\int D[\vec{f}(t')]G[\vec{f}] = \int_{-\infty}^{\infty} \cdots \int_{-\infty}^{\infty} G[\vec{f}] \prod_{t'} d\vec{f}(t'). \tag{2.8}$$

Eq. 2.1 is enforced for all subsequent times $t \geq t' > t_0$, where t is the time for which we would like to calculate averages, for each $\vec{R}_n^{(l)}(t')$. This is done, for a given noise realization $\vec{f}_n^{(l)}(t')$, by virtue of delta functions in the functional integral where we have used the delta functional

$$\delta[\vec{R}_n^{(l)}(t') - \bar{\vec{R}}_n^{(l)}(t')] = \prod_{t \geq t' > t_0} \delta(\vec{R}_n^{(l)}(t') - \bar{\vec{R}}_n^{(l)}(t')) \tag{2.9}$$

and where $\bar{\vec{R}}_n^{(l)}(t')$ satisfies Eq. 2.1 for the given noise realization. We may replace the argument of the delta function as follows:

$$
\begin{aligned}
Z_f(t|t_0) \;=\; & \int \prod_l \left(\prod_n \{ d\vec{R}_n^{(l)}(t_0) \} P_0(\{\vec{R}_n^{(l)}(t_0)\}, t_0) \right) \int \prod_{l,n} \left\{ D\left[\vec{R}_n^{(l)}(t')\right] \times \right. \\
& \delta \left[\frac{\partial \vec{R}_n^{(l)}(t')}{\partial t'} - \frac{1}{\zeta_0} \vec{F}_n^{(l)}(t') - \frac{1}{\zeta_0} \vec{F}_{ext}(\vec{R}_n^{(l)}(t')) \right. \\
& - \frac{1}{\zeta_0} \sum_{l'} \sum_m \vec{F}_{int} \left(\vec{R}_n^{(l)}(t'), \vec{R}_m^{(l')}(t') \right) \\
& \left. \left. - \frac{1}{\zeta_0} \vec{f}_n^{(l)}(t') \right] \right\} J[\vec{R}_n^{(l)}(t')]
\end{aligned}
\tag{2.10}
$$

where the zeroes of the new argument are given by $\vec{R}_n^{(l)}(t') = \bar{\vec{R}}_n^{(l)}(t')$. The transformation of the argument of the delta function introduces the Jacobian $J[\vec{R}_n^{(l)}(t')]$ [33]. This functional integral is a sum over all polymer trajectories that obey the initial condition and the equations of motion, for the given noise realization. It will ultimately play the role of a dynamical partition function in that it, once the noise is averaged over, will be used to perform averages of quantities that depend on the polymer trajectories.

Invoking the Fourier-transform representation of the delta function, we may write:

$$
\begin{aligned}
\delta \left(\frac{\partial \vec{R}_n^{(l)}(t')}{\partial t'} - \frac{1}{\zeta_0} \vec{F}_n^{(l)}(t') - \frac{1}{\zeta_0} \vec{F}_{ext}(\vec{R}_n^{(l)}(t')) - \frac{1}{\zeta_0} \sum_{l'} \sum_m \vec{F}_{int}(\vec{R}_n^{(l)}(t'), \vec{R}_m^{(l')}(t')) \right. \\
\left. - \frac{1}{\zeta_0} \vec{f}_n^{(l)}(t') \right) = \int d\hat{\vec{R}}_n^{(l)}(t') \exp \left[i \hat{\vec{R}}_n^{(l)}(t') \cdot \left(\frac{\partial \vec{R}_n^{(l)}(t')}{\partial t'} - \frac{1}{\zeta_0} \vec{F}_n^{(l)}(t') \right. \right. \\
\left. \left. - \frac{1}{\zeta_0} \vec{F}_{ext}(\vec{R}_n^{(l)}(t')) - \frac{1}{\zeta_0} \sum_{l'} \sum_m \vec{F}_{int}(\vec{R}_n^{(l)}(t'), \vec{R}_m^{(l')}(t')) - \frac{1}{\zeta_0} \vec{f}_n^{(l)}(t') \right) \right] .
\end{aligned}
\tag{2.11}
$$

In doing so, we introduce the variables $\hat{\vec{R}}_n^{(l)}(t')$ which are conjugate to $\vec{R}_n^{(l)}(t')$. One of the advantages of the functional integral approach [33] as opposed to the original MSR formalism [27] is that in the MSR formalism the variables $\hat{\vec{R}}_n^{(l)}(t')$ must be introduced

ad hoc, whereas in the functional integral formalism they arise naturally. We may now average over the Gaussian noise (see Appendix B.1) to give the noise-averaged functional integral $Z(t|t_0) = \langle Z_f(t|t_0)\rangle_f$. The result is

$$\begin{aligned} Z(t|t_0) &= \int \prod_l \left(\prod_n \{d\vec{R}_n^{(l)}(t_0)\} P_0(\{\vec{R}_n^{(l)}(t_0)\}, t_0) \right) \int \prod_{l,n} \left\{ D[\vec{R}_n^{(l)}(t')] D[\hat{\vec{R}}_n^{(l)}(t')] \right\} \\ &\times \exp\left[\sum_{l,n} \int_{t_0}^{t} dt'\, i\hat{\vec{R}}_n^{(l)}(t') \cdot \left(\frac{\partial \vec{R}_n^{(l)}(t')}{\partial t'} - \frac{1}{\zeta_0}\vec{F}_n^{(l)}(t') - \frac{1}{\zeta_0}\vec{F}_{ext}(\vec{R}_n^{(l)}(t')) \right.\right. \\ &- \left.\left. \frac{1}{\zeta_0} \sum_{l',m} \vec{F}_{int}(\vec{R}_n^{(l)}(t'), \vec{R}_m^{(l')}(t')) + \frac{ik_BT}{\zeta_0} \hat{\vec{R}}_n^{(l)}(t') \right) \right] \\ &\times J[\vec{R}_n^{(l)}(t')]. \end{aligned} \tag{2.12}$$

It turns out that the variables $\hat{\vec{R}}_n^{(l)}(t')$ serve as generators of response functions. If we introduce a perturbation to the system by applying a force field $\vec{g}_n^{(l)}(t')$ to the beads, it will produce an extra term in the argument of the exponential in Eq. 2.12 given by $-\sum_{l,n} \int_{t_0}^{t} dt' \, \frac{i}{\zeta_0} \hat{\vec{R}}_n^{(l)}(t') \cdot \vec{g}_n^{(l)}(t')$. The linear response of $\left\langle \vec{R}_n^{(l')}(t') \right\rangle$ to the perturbation $\vec{g}_m^{(l'')}(t'')$ is thus given by

$$\left. \frac{\delta \left\langle R_{\alpha,n}^{(l')}(t') \right\rangle}{\delta g_{\beta,m}^{(l'')}(t'')} \right|_{\vec{g}=0} = -\frac{i}{\zeta_0} \left\langle \hat{R}_{\beta,m}^{(l'')}(t'') \cdot R_{\alpha,n}^{(l')}(t') \right\rangle. \tag{2.13}$$

The form of the Jacobian $J[\vec{R}_n^{(l)}(t')]$ depends on the manner in which the equation of motion is discretized in time. We follow the prescription of Jensen [33] (which is also used by Fredrickson and Helfand [30]) and choose a discretization such that the Jacobian is independent of $\vec{R}_n^{(l)}(t')$. As a result the Jacobian contributes a divergent constant to $Z(t|t_0)$, which will be cancelled by an equivalent divergent constant in the denominator of any average that we choose to calculate since $Z(t|t_0)$ will always appear in the denominator. The constant itself is thus inconsequential and it will be omitted entirely in what follows.

However, the choice of discretization also presents a time-ordering ambiguity issue when taking averages of quantities involving products of $\hat{\vec{R}}_n^{(l)}(t')$ (for example, response functions). Since $\hat{\vec{R}}_n^{(l)}(t')$ generates response functions, any average involving products of $\hat{\vec{R}}_n^{(l)}(t'')$ and $\vec{R}_n^{(l)}(t')$ should be zero if $t'' > t'$. This is an expression of the fact that the response of the system at time t' to perturbations at times $t'' > t'$ must vanish due to causality; such is the case in Eq. 2.13 above. The ambiguity appears when one wishes to calculate the average of an equal-time quantity such as $\hat{\vec{R}}_n^{(l)}(t') \cdot \vec{R}_n^{(l)}(t')$. Here it is unclear as to whether or not the perturbation comes after the response. Jensen resolves this ambiguity by enforcing that, for any such averages, the discrete time argument of $\hat{\vec{R}}_n^{(l)}(t')$ be displaced to an infinitesimally later time, meaning the average is zero [33]. In general, if t' is the latest time appearing in the average, any product containing $\hat{\vec{R}}_n^{(l)}(t')$ must average to zero.

2.3 Introduction of collective field variables

We have constructed a functional integral $Z(t|t_0)$ that serves much the same function in this dynamical theory as the partition function does in the development of equilibrium self-consistent field theory (SCFT). This is the first of many similarities between the structure of the two theories, and to help emphasize the analogy between the two, Appendix A gives a concise review of equilibrium self-consistent field theory. It becomes convenient in the subsequent development of the theory (much like in equilibrium SCFT) to write the functional integral $Z(t|t_0)$ in terms of collective field variables such as the density field. The choice of collective field variables is motivated by the problem being studied and by the properties one is interested in examining. For example, the density field would be a poor choice if one is interested in the orientational alignment of rodlike polymers; rather, a collective field variable that contains information about the direction of the chain backbone would be appropriate. This

additional flexibility is powerful and broadens the applicability of the theory, but this thesis will develop the theory in the context of the time-dependent density field. We introduce two collective fields, the density field

$$\hat{\rho}(\vec{r},t) = \sum_{l,n} \delta(\vec{r} - \vec{R}_n^{(l)}(t)), \tag{2.14}$$

and a vector "response density" field

$$\hat{\boldsymbol{\phi}}(\vec{r},t) = \sum_{l,n} \hat{\vec{R}}_n^{(l)}(t)\delta(\vec{r} - \vec{R}_n^{(l)}(t)). \tag{2.15}$$

Using these definitions we may re-express several terms in $Z(t|t_0)$ in terms of the collective field variables, specifically

$$\sum_{l,n} \int_{t_0}^{t} dt'\, i\hat{\vec{R}}_n^{(l)}(t') \cdot \vec{F}_{ext}(\vec{R}_n^{(l)}(t')) = i \int d\vec{r} \int_{t_0}^{t} dt'\, \hat{\boldsymbol{\phi}}(\vec{r},t') \cdot \vec{F}_{ext}(\vec{r}) \tag{2.16}$$

and

$$\begin{aligned} \sum_{l,n} \int_{t_0}^{t} dt'\, i\hat{\vec{R}}_n^{(l)}(t') \quad \cdot \quad & \sum_{l',m} \vec{F}_{int}(\vec{R}_n^{(l)}(t'), \vec{R}_m^{(l')}(t')) \\ = \; & i \int d\vec{r} \int_{t_0}^{t} dt'\, \hat{\boldsymbol{\phi}}(\vec{r},t') \cdot \sum_{l',m} \vec{F}_{int}(\vec{r}, \vec{R}_m^{(l')}(t')) \\ = \; & i \int d\vec{r} \int d\vec{r}' \int_{t_0}^{t} dt'\, \hat{\rho}(\vec{r}',t')\hat{\boldsymbol{\phi}}(\vec{r},t') \cdot \vec{F}_{int}(\vec{r},\vec{r}'). \end{aligned} \tag{2.17}$$

Motivated by our desire to express $Z(t|t_0)$ in terms of field variables that do not depend explicitly on particle positions $\vec{R}_n^{(l)}(t')$, we introduce two field variables $\rho(\vec{r},t')$ and $\boldsymbol{\phi}(\vec{r},t')$. This is a coarse-graining procedure wherein the hatted collective field variables $\hat{\rho}(\vec{r},t')$ and $\hat{\boldsymbol{\phi}}(\vec{r},t')$ are replaced everywhere in $Z(t|t_0)$ by $\rho(\vec{r},t')$ and $\boldsymbol{\phi}(\vec{r},t')$

provided that we insert the identities

$$1 = \int D[\rho]\delta[\rho - \hat{\rho}] \tag{2.18}$$

and

$$1 = \int D[\boldsymbol{\phi}]\delta[\boldsymbol{\phi} - \hat{\boldsymbol{\phi}}], \tag{2.19}$$

where the functional integrals are over space and time:

$$\int D[\rho]G[\rho] = \int_{-\infty}^{\infty} \cdots \int_{-\infty}^{\infty} G[\rho] \prod_{\vec{r},t} d\rho(\vec{r},t). \tag{2.20}$$

By again invoking the Fourier-transform representation of the delta functional,

$$\int D[\rho]\delta\left[\rho - \hat{\rho}\right] = \int D[\rho]D[\omega] \exp\left[\int d\vec{r} \int_{t_0}^{t} dt'\, i\omega(\vec{r},t')\left(\rho(\vec{r},t') - \hat{\rho}(\vec{r},t')\right)\right] \tag{2.21}$$

and

$$\int D[\boldsymbol{\phi}]\delta\left[\boldsymbol{\phi} - \hat{\boldsymbol{\phi}}\right] = \int D[\boldsymbol{\phi}]D[\boldsymbol{\psi}] \exp\left[\int d\vec{r} \int_{t_0}^{t} dt'\, i\boldsymbol{\psi}(\vec{r},t') \cdot \left(\boldsymbol{\phi}(\vec{r},t') - \hat{\boldsymbol{\phi}}(\vec{r},t')\right)\right], \tag{2.22}$$

we introduce two further field variables $\omega(\vec{r},t')$ and $\boldsymbol{\psi}(\vec{r},t')$. The functional integral can now be written as an integral over the collective fields

$$Z(t|t_0) = \int D[\rho]D[\omega]D[\boldsymbol{\phi}]D[\boldsymbol{\psi}]e^{-L[\rho,\omega,\boldsymbol{\phi},\boldsymbol{\psi}]}. \tag{2.23}$$

$L[\rho,\omega,\boldsymbol{\phi},\boldsymbol{\psi}]$ is a functional of the four fields $\rho(\vec{r},t')$, $\omega(\vec{r},t')$, $\boldsymbol{\phi}(\vec{r},t')$ and $\boldsymbol{\psi}(\vec{r},t')$ and will be referred to as the *effective action*. It has the form

$$\begin{aligned} L[\rho,\omega,\boldsymbol{\phi},\boldsymbol{\psi}] &= -i\int d\vec{r}\int_{t_0}^{t} dt'\ (\boldsymbol{\phi}(\vec{r},t')\cdot\boldsymbol{\psi}(\vec{r},t')+\omega(\vec{r},t')\rho(\vec{r},t')) \\ &+ i\int d\vec{r}\int_{t_0}^{t} dt'\ \left(\frac{1}{\zeta_0}\boldsymbol{\phi}(\vec{r},t')\cdot\vec{F}_{ext}(\vec{r})+\frac{1}{\zeta_0}\int d\vec{r}'\,\rho(\vec{r}',t')\boldsymbol{\phi}(\vec{r},t')\cdot\vec{F}_{int}(\vec{r},\vec{r}')\right) \\ &- \ln Q_{n_P}([\omega,\boldsymbol{\psi}],t|t_0). \end{aligned} \tag{2.24}$$

The interpretation of $\boldsymbol{\phi}(\vec{r},t)$, similar to that of $\hat{\vec{R}}_n^{(l)}(t)$, is that it is a generator of response functions. If we again introduce some external perturbation to the system by applying a force $\vec{g}(\vec{r},t')$, it will produce an extra term in the effective action given by $i\int d\vec{r}\int dt'\frac{1}{\zeta_0}\boldsymbol{\phi}(\vec{r},t')\cdot\vec{g}(\vec{r},t')$. The linear response of the average density $\langle\rho(\vec{r},t')\rangle$ to a perturbation at $\vec{r}'$ and t'' is given by

$$\frac{\delta\langle\rho(\vec{r},t')\rangle}{\delta\vec{g}(\vec{r}',t'')}=\frac{i}{\zeta_0}\langle\rho(\vec{r},t')\boldsymbol{\phi}(\vec{r}',t'')\rangle\,. \tag{2.25}$$

$Q_{n_P}([\omega,\boldsymbol{\psi}],t|t_0)$ contains the terms that remain explicitly dependent on bead positions, and has the form

$$\begin{aligned} Q_{n_P}([\omega,\boldsymbol{\psi}],t|t_0) &= \int\prod_l\left(\prod_n\{d\vec{R}_n^{(l)}(t_0)\}P_0(\{\vec{R}_n^{(l)}(t_0)\},t_0)\right)\int\prod_{l,n}\Big\{D[\vec{R}_n^{(l)}(t')] \\ &\times\ D[\hat{\vec{R}}_n^{(l)}(t')]\Big\}\exp\left(\sum_{l,n}\int_{t_0}^{t}dt'\,i\hat{\vec{R}}_n^{(l)}(t')\cdot\left(\frac{\partial\vec{R}_n^{(l)}(t')}{\partial t'}-\frac{1}{\zeta_0}\vec{F}_n^{(l)}(t')\right.\right. \\ &-\ \left.\left.\boldsymbol{\psi}(\vec{R}_n^{(l)}(t'),t')+\frac{ik_BT}{\zeta_0}\hat{\vec{R}}_n^{(l)}(t')\right)-i\sum_{l,n}\int_{t_0}^{t}dt'\,\omega(\vec{R}_n^{(l)}(t'),t')\right). \end{aligned} \tag{2.26}$$

Note that the square brackets in the argument of $Q_{n_P}([\omega,\boldsymbol{\psi}],t|t_0)$ mean that it is a *functional* of $\omega(\vec{r},t')$ and $\boldsymbol{\psi}(\vec{r},t')$ but simply a *function* of t and t_0. $Q_{n_P}([\omega,\boldsymbol{\psi}],t|t_0)$ is

a product of n_P decoupled *dynamical single-chain partition functions* $Q([\omega,\boldsymbol{\psi}],t|t_0)$

$$\begin{aligned} Q([\omega,\boldsymbol{\psi}],t|t_0) &= \int\prod_n\{d\vec{R}_n(t_0)\}P_0(\{\vec{R}_n(t_0)\},t_0)\int\prod_n\left\{D[\vec{R}_n(t')]D[\hat{\vec{R}}_n(t')]\right\} \\ &\times \exp\left(\sum_n\int_{t_0}^t dt'\,i\hat{\vec{R}}_n(t')\cdot\left(\frac{\partial\vec{R}_n(t')}{\partial t'}-\frac{1}{\zeta_0}\vec{F}_n(t')-\boldsymbol{\psi}(\vec{R}_n(t'),t')\right.\right. \\ &+ \left.\left.\frac{ik_BT}{\zeta_0}\hat{\vec{R}}_n(t')\right)-\sum_n\int_{t_0}^t dt'\,i\omega(\vec{R}_n(t'),t')\right), \end{aligned} \tag{2.27}$$

and can be factored accordingly:

$$Q_{n_P}([\omega,\boldsymbol{\psi}],t|t_0)=Q([\omega,\boldsymbol{\psi}],t|t_0)^{n_P}. \tag{2.28}$$

$Q([\omega,\boldsymbol{\psi}],t|t_0)$ is the dynamical functional integral for a single chain that would be obtained from a Langevin equation in an external force field $\boldsymbol{\psi}$, with the peculiar addition of the field ω which can be interpreted as a generator of density correlation functions (for a discussion of this, see Appendix B.5). The analog to $Q([\omega,\boldsymbol{\psi}],t|t_0)$ in the equilibrium theory is simply called the *single-chain partition function.* The effective action now takes the form

$$\begin{aligned} L[\rho,\omega,\boldsymbol{\phi},\boldsymbol{\psi}] &= -i\int d\vec{r}\int_{t_0}^t dt'\,\left(\boldsymbol{\phi}(\vec{r},t')\cdot\boldsymbol{\psi}(\vec{r},t')+\omega(\vec{r},t')\rho(\vec{r},t')\right) \\ &+ i\int d\vec{r}\int_{t_0}^t dt'\,\left(\frac{1}{\zeta_0}\boldsymbol{\phi}(\vec{r},t')\cdot\vec{F}_{ext}(\vec{r})+\frac{1}{\zeta_0}\int d\vec{r}'\,\rho(\vec{r}',t')\boldsymbol{\phi}(\vec{r},t')\cdot\vec{F}_{int}(\vec{r},\vec{r}')\right) \\ &- n_P\ln Q([\omega,\boldsymbol{\psi}],t|t_0). \end{aligned} \tag{2.29}$$

$L[\rho,\omega,\boldsymbol{\phi},\boldsymbol{\psi}]$ bears resemblance to the free energy functional in equilibrium self-consistent field theory, in that it may be separated into terms containing the fields and their conjugates, interaction terms and the single-chain partition function as in Eq. 2.29. This essentially completes the description of the *exact* functional integral $Z(t|t_0)$. Due to the complicated nature of $Z(t|t_0)$, it must be treated within some

approximation. Fredrickson and Helfand [30] performed a Gaussian approximation to $Q([\omega, \boldsymbol{\psi}], t|t_0)$, truncating the action to quadratic order in ρ, ω, $\boldsymbol{\phi}$ and $\boldsymbol{\psi}$. Vilgis [31] performed a self-consistent Hartree approximation which also expresses the action as a Gaussian-type functional. We will take a different approach, by employing a dynamical saddle-point approximation while treating the single-chain dynamics ($Q([\omega, \boldsymbol{\psi}], t|t_0)$) exactly (within the mean-field approximation: that is, the dynamics being *exactly* that of a single chain interacting with the mean fields $\boldsymbol{\psi}$ and ω). With $Z(t|t_0)$ written as above in terms of the dynamical single-chain partition function $Q([\omega, \boldsymbol{\psi}], t|t_0)$, the single-chain dynamics is made handily explicit in $Z(t|t_0)$. This conveniently sets up the analysis using self-consistent mean-field methods (the main result of this thesis and the topic of the next chapter) in a way that is analogous to what is done in equilibrium SCFT.

Chapter 3

The dynamical self-consistent field-theoretic formalism

Up to this point, the treatment of $Z(t|t_0)$ has been exact. In order to make further progress, the mean-field approximation will be applied to $Z(t|t_0)$. Ultimately, this approximation treats the problem no longer as n_P polymers interacting with each other directly but as n_P polymers interacting individually with a *mean field* that approximates the interaction between polymers. In doing so we reduce the interacting many-body problem to the problem of a single chain evolving under the influence of the mean field. The single-chain dynamics will still be treated exactly (within the mean-field approximation), which amounts to us requiring a method to calculate $Q([\omega, \boldsymbol{\psi}], t|t_0)$ exactly. In equilibrium SCFT, the analogous single-chain partition function is calculated by establishing a relationship between the single-chain partition function and a single-chain propagator, which satisfies a *modified diffusion equation* (see Appendix A). We will show that a similar approach can be used for the calculation of the dynamical single-chain partition function.

This chapter can be separated into two sections: first, the exact treatment of the dynamical single-chain partition function $Q([\omega, \boldsymbol{\psi}], t|t_0)$, which stands on its own and

holds whether or not the mean-field approximation is applied. The second section consists of the mean-field approximation to the exact field theory and the mean-field equations that result from it.

3.1 Exact treatment of the dynamical single-chain partition function

The dynamical single-chain partition function can be written in terms of a propagator that satisfies an equation similar to a Fokker-Planck equation. We begin with $Q([\omega, \boldsymbol{\psi}], t|t_0)$, which can itself be interpreted (if $\omega = 0$) as the noise-averaged dynamical partition function for a single chain moving in an external force field $\zeta_0 \boldsymbol{\psi}$

$$\begin{aligned} Q([\omega, \boldsymbol{\psi}], t|t_0) &= \int \prod_n \{d\vec{R}_n(t_0)\} P_0(\{\vec{R}_n(t_0)\}, t_0) \int \prod_n \left\{ D[\vec{R}_n(t')] D[\hat{\vec{R}}_n(t')] \right\} \\ &\times \exp\left(\sum_n \int_{t_0}^{t} dt'\, i\hat{\vec{R}}_n(t') \cdot \left(\frac{\partial \vec{R}_n(t')}{\partial t'} - \frac{1}{\zeta_0} \vec{F}_n(t') - \boldsymbol{\psi}(\vec{R}_n(t'), t') \right.\right. \\ &+ \left.\left. \frac{i k_B T}{\zeta_0} \hat{\vec{R}}_n(t') \right) - \sum_n \int_{t_0}^{t} dt'\, i\omega(\vec{R}_n(t'), t') \right). \end{aligned} \tag{3.1}$$

By discretizing $Q([\omega, \boldsymbol{\psi}], t|t_0)$ in time (see Appendix B.2), we may formulate this integral iteratively by defining the quantity $q(\{\vec{r}_n\}, t_i|t_0)$, where we have relabeled $\vec{R}_n(t_i)$ as $\vec{r}_n$ for convenience. This replacement is unambiguous because the context in which it is used (as an argument of $q(\{\vec{r}_n\}, t_i|t_0)$) makes it clear that $\vec{r}_n$ is defined at time t_i. The quantity $q(\{\vec{r}_n\}, t_i|t_0)$ satisfies

$$Q([\omega, \boldsymbol{\psi}], t|t_0) = \int \prod_n \{d\vec{r}_n\} q(\{\vec{r}_n\}, t|t_0) \tag{3.2}$$

and

$$q(\{\vec{r}_n\}, t_0|t_0) = P_0(\{\vec{r}_n\}, t_0), \tag{3.3}$$

as well as the recursive relationship

$$\begin{aligned} q(\{\vec{r}_n\}, t_{i+1}|t_0) &= \exp\left(-\sum_n \Delta t i\omega(\vec{r}_n, t_{i+1})\right) \int \prod_n \left\{d\hat{\vec{r}}_n d\vec{r}'_n\right\} \\ &\times \exp\left\{\sum_n i\hat{\vec{r}}_n \cdot \left(\vec{r}_n - \vec{r}'_n - \frac{\Delta t}{\zeta_0}\vec{F}_n(t_{i+1})\right.\right. \\ &- \left.\left. \Delta t\boldsymbol{\psi}(\vec{r}_n, t_{i+1}) + \frac{i\Delta t k_B T}{\zeta_0}\hat{\vec{r}}_n\right)\right\} q(\{\vec{r}'_n\}, t_i|t_0) \end{aligned} \tag{3.4}$$

for $i = 0, \ldots, K-1$, where $t_i = t_0 + i\Delta t$ and $t_K = t$. The modified Fokker-Planck equation can be derived from Eq. 3.4. This derivation is detailed in Appendix B.3, and the result is

$$\begin{aligned} \frac{\partial q(\{\vec{r}_n\}, t|t_0)}{\partial t} &= \frac{k_B T}{\zeta_0} \sum_n \nabla^2_{\vec{r}_n} q(\{\vec{r}_n\}, t|t_0) \\ &- \sum_n \nabla_{\vec{r}_n} \cdot \left(\frac{1}{\zeta_0}\vec{F}_n(t) q(\{\vec{r}_n\}, t|t_0)\right) \\ &- \sum_n \nabla_{\vec{r}_n} \cdot [\boldsymbol{\psi}(\vec{r}_n, t) q(\{\vec{r}_n\}, t|t_0)] \\ &- i\left[\sum_n \omega(\vec{r}_n, t)\right] q(\{\vec{r}_n\}, t|t_0). \end{aligned} \tag{3.5}$$

We have derived an evolution equation for the functional $q(\{\vec{r}_n\}, t|t_0)$. Eqs. 3.2, 3.3 and 3.5 provide us with a prescription to calculate $Q([\omega, \boldsymbol{\psi}], t|t_0)$ exactly, and they constitute the first significant result of this thesis. In the simple case of a Brownian particle instead of a chain ($N = 1$, $\vec{F}_n(t) = 0$), this evolution equation reduces to

$$\frac{\partial q(\vec{r}, t|t_0)}{\partial t} = \frac{k_B T}{\zeta_0}\nabla^2 q(\vec{r}, t|t_0) - \nabla \cdot (\boldsymbol{\psi}(\vec{r}, t) q(\vec{r}, t|t_0)) - i\omega(\vec{r}, t) q(\vec{r}, t|t_0), \tag{3.6}$$

which is the well-known Fokker-Planck equation with the addition of the term containing the 'source' field ω. For comparison, in the $N = 2$ case

$$\begin{aligned}\frac{\partial q(\vec{r}_1,\vec{r}_2,t|t_0)}{\partial t} &= \frac{k_BT}{\zeta_0}\left(\nabla^2_{\vec{r}_1}+\nabla^2_{\vec{r}_2}\right)q(\vec{r}_1,\vec{r}_2,t|t_0)\\ &- \nabla_{\vec{r}_1}\cdot\left(\frac{1}{\zeta_0}\vec{F}_1(t)q(\vec{r}_1,\vec{r}_2,t|t_0)\right)-\nabla_{\vec{r}_2}\cdot\left(\frac{1}{\zeta_0}\vec{F}_2(t)q(\vec{r}_1,\vec{r}_2,t|t_0)\right)\\ &- \nabla_{\vec{r}_1}\cdot(\boldsymbol{\psi}(\vec{r}_1,t)q(\vec{r}_1,\vec{r}_2,t|t_0))-\nabla_{\vec{r}_2}\cdot(\boldsymbol{\psi}(\vec{r}_2,t)q(\vec{r}_1,\vec{r}_2,t|t_0))\\ &- i\left[\omega(\vec{r}_1,t)+\omega(\vec{r}_2,t)\right]q(\vec{r}_1,\vec{r}_2,t|t_0). \qquad (3.7)\end{aligned}$$

We interpret $q(\{\vec{r}_n\},t|t_0)$ as the (non-normalized) probability distribution functional for the single chain; that is, $q(\{\vec{r}_n\},t|t_0)$ is proportional to the probability that the single chain has the conformation given by $\{\vec{r}_n\}$ at time t given that its initial conformation at time t_0 is described by the probability distribution $P_0(\{\vec{r}_n\},t_0)$. We would expect such a conditional probability distribution to possess the multiplicative property

$$q(\{\vec{r}_n\},t|t_0)=\int\prod_n\{d\vec{r}'_n\}q(\{\vec{r}_n\},t|\{\vec{r}'_n\},t')q(\{\vec{r}'_n\},t'|t_0). \qquad (3.8)$$

This states that the probability of finding the chain in the conformation $\{\vec{r}_n\}$ at time t (provided that its initial conformation satisfied the probability distribution $P_0(\{\vec{r}''_n\},t_0)$ at time t_0) can be written as a sum over *intermediate* conformations $\{\vec{r}'_n\}$ at time t' ($t > t' > t_0$) of the product of the probabilities that a) the conformation be $\{\vec{r}_n\}$ at time t provided that the conformation was $\{\vec{r}'_n\}$ at t' and b) the conformation be $\{\vec{r}'_n\}$ at time t' provided that the initial conformation satisfied the probability distribution $P_0(\{\vec{r}''_n\},t_0)$. A derivation of Eq. 3.8 is provided in Appendix B.4. We refer to $q(\{\vec{r}_n\},t|\{\vec{r}'_n\},t')$ as the *single-chain propagator* as it is proportional to the probability for the chain to evolve or *propagate* from one conformation to another in a given time, with the proportionality constant equal to $Q([\omega,\boldsymbol{\psi}],t|t')$. We may calculate the probability of finding the chain in a particular conformation $\{\vec{r}_n\}$ at

time t by $P(\{\vec{r}_n\},t) = \left\langle \prod_n \delta(\vec{r}_n - \vec{R}_n(t)) \right\rangle$. Inserting $\prod_n \delta(\vec{r}_n - \vec{R}_n(t))$ into Eq. 3.1, the result is

$$P(\{\vec{r}_n\},t) = \frac{q(\{\vec{r}_n\},t|t_0)}{Q([\omega,\boldsymbol{\psi}],t|t_0)}. \tag{3.9}$$

The properties demonstrated by Eq. 3.8 and 3.9 will prove useful for interpreting the mean-field equations in the next section.

3.2 The mean-field approximation

A method of calculating the single-chain partition function exactly has been shown. The mean-field approximation to $Z(t|t_0)$ will now be made. $Z(t|t_0)$ is approximated by the value or values of its integrand at the extrema of $L[\rho,\omega,\boldsymbol{\phi},\boldsymbol{\psi}]$. The conditions that the action be an extremum are

$$\frac{\delta L[\rho,\omega,\boldsymbol{\phi},\boldsymbol{\psi}]}{\delta\rho(\vec{r},t)} = 0 \tag{3.10}$$

$$\frac{\delta L[\rho,\omega,\boldsymbol{\phi},\boldsymbol{\psi}]}{\delta\omega(\vec{r},t)} = 0 \tag{3.11}$$

$$\frac{\delta L[\rho,\omega,\boldsymbol{\phi},\boldsymbol{\psi}]}{\delta\phi_\alpha(\vec{r},t)} = 0 \tag{3.12}$$

$$\frac{\delta L[\rho,\omega,\boldsymbol{\phi},\boldsymbol{\psi}]}{\delta\psi_\alpha(\vec{r},t)} = 0 \tag{3.13}$$

These conditions lead to the set of mean-field equations

$$\omega(\vec{r},t) = \frac{1}{\zeta_0}\int d\vec{r'}\,\boldsymbol{\phi}(\vec{r'},t)\cdot\vec{F}_{int}(\vec{r'},\vec{r}) \tag{3.14}$$

$$\rho(\vec{r},t) = -n_P\frac{\delta \ln Q([\omega,\psi],t|t_0)}{\delta i\omega(\vec{r},t)} \tag{3.15}$$

$$\psi_\alpha(\vec{r},t) = \frac{1}{\zeta_0}F_{ext,\alpha}(\vec{r}) + \frac{1}{\zeta_0}\int d\vec{r'}\,\rho(\vec{r'},t)F_{int,\alpha}(\vec{r},\vec{r'}) \tag{3.16}$$

$$\phi_\alpha(\vec{r},t) = -n_P\frac{\delta \ln Q([\omega,\psi],t|t_0)}{\delta i\psi_\alpha(\vec{r},t)} \tag{3.17}$$

Eq. 3.15 suggests that functional derivatives of $Q([\omega, \boldsymbol{\psi}], t|t_0)$ with respect to ω generate density correlation functions (see Appendix B.5 for a discussion of this). We interpret $\boldsymbol{\psi}$ as the mean field, since according to Eq. 3.16 it contains the external force field as well as the second term which contains an average of $\vec{F}_{int}$, weighted by the mean density ρ.

3.3 Functional derivatives of $Q([\omega, \boldsymbol{\psi}], t|t_0)$

To proceed further, the functional derivatives appearing in Eqs. 3.15 and 3.17 must be evaluated. It is most convenient to evaluate the functional derivatives of $Q([\omega, \boldsymbol{\psi}], t|t_0)$ in terms of the single-chain propagator $q(\{\vec{r}_n\}, t|t_0)$, because ultimately $q(\{\vec{r}_n\}, t|t_0)$ is the quantity more accessible to us (through the functional Fokker-Planck equation). In Eq. 3.15 we have

$$\begin{aligned}
\rho(\vec{r}', t) &= -n_P \frac{\delta \ln Q([\omega, \boldsymbol{\psi}], t|t_0)}{\delta i\omega(\vec{r}', t)} \\
&= -\frac{n_P}{Q([\omega, \boldsymbol{\psi}], t|t_0)} \frac{\delta Q([\omega, \boldsymbol{\psi}], t|t_0)}{\delta i\omega(\vec{r}', t)} \\
&= -\frac{n_p}{Q([\omega, \boldsymbol{\psi}], t|t_0)} \int \prod_n \{d\vec{r}_n\} \frac{\delta q(\{\vec{r}_n\}, t|t_0)}{\delta i\omega(\vec{r}', t)}.
\end{aligned} \tag{3.18}$$

The propagator satisfies the modified Fokker-Planck equation, Eq. 3.5. Taking the functional derivative with respect to $\omega(\vec{r}',t)$ of this equation gives

$$\begin{aligned}\frac{\partial}{\partial t'}\frac{\delta q(\{\vec{r}_n\},t'|t_0)}{\delta i\omega(\vec{r}',t)} &= \frac{k_BT}{\zeta_0}\sum_n \nabla^2_{\vec{r}_n}\frac{\delta q(\{\vec{r}_n\},t'|t_0)}{\delta i\omega(\vec{r}',t)} \\ &- \sum_n \nabla_{\vec{r}_n}\cdot\left(\frac{1}{\zeta_0}\vec{F}_n(t')\frac{\delta q(\{\vec{r}_n\},t'|t_0)}{\delta i\omega(\vec{r}',t)}\right) \\ &- \sum_n \nabla_{\vec{r}_n}\cdot\left(\boldsymbol{\psi}(\vec{r}_n,t')\frac{\delta q(\{\vec{r}_n\},t'|t_0)}{\delta i\omega(\vec{r}',t)}\right) \\ &- \delta(t-t')\left[\sum_n \delta(\vec{r}'-\vec{r}_n)\right] q(\{\vec{r}_n\},t'|t_0) \\ &- i\left[\sum_n \omega(\vec{r}_n,t')\right]\frac{\delta q(\{\vec{r}_n\},t'|t_0)}{\delta i\omega(\vec{r}',t)}. \end{aligned} \tag{3.19}$$

We define the operator

$$\begin{aligned}\hat{\mathcal{O}} &= \frac{\partial}{\partial t'} - \sum_n \left\{\frac{k_BT}{\zeta_0}\nabla^2_{\vec{r}_n} - \nabla_{\vec{r}_n}\cdot[\boldsymbol{\psi}(\vec{r}_n,t')(\ldots)]\right. \\ &- \left.\nabla_{\vec{r}_n}\cdot\left[\frac{1}{\zeta_0}\vec{F}_n(t')(\ldots)\right] - i\omega(\vec{r}_n,t')\right\} \end{aligned} \tag{3.20}$$

and write

$$\hat{\mathcal{O}}\frac{\delta q(\{\vec{r}_n\},t'|t_0)}{\delta i\omega(\vec{r}',t)} = -\delta(t-t')\sum_m \delta(\vec{r}'-\vec{r}_m)q(\{\vec{r}_n\},t'|t_0). \tag{3.21}$$

The functional derivative will be calculated using a Green's function approach. We seek a Green's function $G(\{\vec{r}_n\},t'|\{\vec{r}''_n\},t'')$ such that

$$\hat{\mathcal{O}}G(\{\vec{r}_n\},t'|\{\vec{r}''_n\},t'') = \delta(t'-t'')\prod_n \delta(\vec{r}_n-\vec{r}''_n) \tag{3.22}$$

Once $G(\{\vec{r}_n\},t'|[\vec{r}''_n\},t'')$ is known, Eq. 3.21 may be solved:

$$\begin{aligned}\frac{\delta q(\{\vec{r}_n\},t'|t_0)}{\delta i\omega(\vec{r}',t)} &= -\int dt'' \int \prod_n \{d\vec{r}''_n\} G(\{\vec{r}_n\},t'|\{\vec{r}''_n\},t'') \\ &\times \delta(t-t'')\sum_m \delta(\vec{r}'-\vec{r}''_m) q(\{\vec{r}''_n\},t''|t_0). \end{aligned} \tag{3.23}$$

The form

$$G(\{\vec{r}_n\},t'|\{\vec{r}''_n\},t'') = \theta(t'-t'')q(\{\vec{r}_n\},t'|\{\vec{r}''_n\},t''), \tag{3.24}$$

can be shown to satisfy Eq. 3.22:

$$\begin{aligned}\hat{\mathcal{O}}G(\{\vec{r}_n\},t'|\{\vec{r}''_n\},t'') &= \delta(t'-t'')q(\{\vec{r}_n\},t'|\{\vec{r}''_n\},t'') + \theta(t'-t'')\hat{\mathcal{O}}q(\{\vec{r}_n\},t'|\{\vec{r}''_n\},t'') \\ &= \delta(t'-t'')q(\{\vec{r}_n\},t'|\{\vec{r}''_n\},t'') \end{aligned} \tag{3.25}$$

where we have used the fact that $q(\{\vec{r}_n\},t'|\{\vec{r}''_n\},t'')$ satisfies the modified functional Fokker-Planck equation and therefore $\hat{\mathcal{O}}q(\{\vec{r}_n\},t'|\{\vec{r}''_n\},t'')=0$. Evaluation of $q(\{\vec{r}_n\},t'|\{\vec{r}''_n\},t'')$ at $t'=t''$ gives $\prod_n \delta(\vec{r}_n-\vec{r}''_n)$, so we have

$$\hat{\mathcal{O}}G(\{\vec{r}_n\},t'|\{\vec{r}''_n\},t'') = \prod_n \delta(\vec{r}_n-\vec{r}''_n)\delta(t'-t''), \tag{3.26}$$

which matches Eq. 3.22 and confirms the choice for $G(\{\vec{r}_n\},t'|\{\vec{r}''_n\},t'')$. The functional derivative is then given by

$$\begin{aligned}
\frac{\delta q(\{\vec{r}_n\},t'|t_0)}{\delta i\omega(\vec{r}',t)} &= -\int dt'' \int \prod_n \{d\vec{r}''_n\}\theta(t'-t'') \\
&\times\ q(\{\vec{r}_n\},t'|\{\vec{r}''_n\},t'')\sum_m \delta(\vec{r}'-\vec{r}''_m)\delta(t-t'') \\
&\times\ q(\{\vec{r}''_n\},t''|t_0) \\
&= -\int_{t_0}^{t'} dt'' \int \prod_n \{d\vec{r}''_n\} q(\{\vec{r}_n\},t'|\{\vec{r}''_n\},t'') \\
&\times\ \delta(t-t'')\sum_m \delta(\vec{r}'-\vec{r}''_m) q(\{\vec{r}''_n\},t''|t_0) \\
&= -\int \prod_n \{d\vec{r}''_n\} q(\{\vec{r}_n\},t'|\{\vec{r}''_n\},t)\sum_m \delta(\vec{r}'-\vec{r}''_m) q(\{\vec{r}''_n\},t|t_0),
\end{aligned} \tag{3.27}$$

for $t' > t$ (it is zero for $t' < t$). In order to calculate the functional derivative of $q(\{\vec{r}_n\},t|t_0)$, we take the limit as $t' \to t^+$ and obtain

$$\begin{aligned}
\frac{\delta q(\{\vec{r}_n\},t|t_0)}{\delta i\omega(\vec{r}',t)} &= -\int \prod_n \{d\vec{r}''_n\} q(\{\vec{r}_n\},t|\{\vec{r}''_n\},t) \\
&\times\ \sum_m \delta(\vec{r}'-\vec{r}''_m) q(\{\vec{r}''_n\},t|t_0) \\
&= -\sum_m \int \prod_n \{d\vec{r}''_n \delta(\vec{r}_n-\vec{r}''_n)\} \\
&\times\ \delta(\vec{r}'-\vec{r}''_m) q(\{\vec{r}''_n\},t|t_0) \\
&= -\sum_m \delta(\vec{r}'-\vec{r}_m) q(\{\vec{r}_n\},t|t_0)
\end{aligned} \tag{3.28}$$

so from Eq. 3.18:

$$\rho(\vec{r},t) = \frac{n_P}{Q([\omega,\boldsymbol{\psi}],t|t_0)}\sum_m \int \prod_n \{d\vec{r}_n\}\delta(\vec{r}-\vec{r}_m) q(\{\vec{r}_n\},t|t_0) \tag{3.29}$$

We can define $q(\vec{r}, m, t|t_0)$

$$q(\vec{r}, m, t|t_0) = \int \prod_n \{d\vec{r}_n\} \delta(\vec{r} - \vec{r}_m) q(\{\vec{r}_n\}, t|t_0) \tag{3.30}$$

which is proportional to the probability of finding the m^{th} chain segment at position $\vec{r}$ at time t. Eq. 3.29 can then be interpreted as a sum over m of such probabilities, giving the total probability (or in this case density) of chain segments at $\vec{r}$ at time t:

$$\rho(\vec{r}, t) = \frac{n_P}{Q([\omega, \boldsymbol{\psi}], t|t_0)} \sum_m q(\vec{r}, m, t|t_0) \tag{3.31}$$

where

$$Q([\omega, \boldsymbol{\psi}], t|t_0) = \int d\vec{r}\, q(\vec{r}, m, t|t_0). \tag{3.32}$$

The functional derivative with respect to $\psi_\alpha(\vec{r}, t)$, appearing in Eq. 3.17, may also be calculated using the same Green's function approach. We may write

$$\hat{\mathcal{O}} \frac{\delta q(\{\vec{r}_n\}, t'|t_0)}{\delta i \psi_\alpha(\vec{r}, t)} = i \sum_m \frac{\partial}{\partial r_{\alpha,m}} \left[\delta(\vec{r} - \vec{r}_m) \delta(t - t') q(\{\vec{r}_n\}, t'|t_0) \right]. \tag{3.33}$$

The calculation proceeds as it did before. Skipping to the step analogous to Eq. 3.28:

$$\begin{aligned} \frac{\delta q(\{\vec{r}_n\}, t'|t_0)}{\delta i \psi_\alpha(\vec{r}, t)} &= i \int \prod_n \{d\vec{r}''_n\} q(\{\vec{r}_n\}, t'|\{\vec{r}''_n\}, t) \\ &\times \sum_m \frac{\partial}{\partial r''_{\alpha,m}} \left[\delta(\vec{r} - \vec{r}''_m) q(\{\vec{r}''_n\}, t|t_0) \right] \end{aligned} \tag{3.34}$$

and we employ integration by parts

$$\begin{aligned} \frac{\delta q(\{\vec{r}_n\}, t'|t_0)}{\delta i \psi_\alpha(\vec{r}, t)} &= -i \sum_m \int \prod_n \{d\vec{r}''_n\} \frac{\partial}{\partial r''_{\alpha,m}} q(\{\vec{r}_n\}, t'|\{\vec{r}''_n\}, t) \\ &\times \delta(\vec{r} - \vec{r}''_m) q(\{\vec{r}''_n\}, t|t_0). \end{aligned} \tag{3.35}$$

From Eq. 3.17:

$$\begin{aligned}\phi_\alpha(\vec{r},t) &= -\frac{in_P}{Q([\omega,\boldsymbol{\psi}],t'|t_0)}\sum_m\int\prod_n\{d\vec{r}''_n\}\delta(\vec{r}-\vec{r}''_m)\\ &\times \frac{\partial}{\partial r''_{\alpha,m}}\left(\int\prod_n\{d\vec{r}_n\}q(\{\vec{r}_n\},t'|\{\vec{r}''_n\},t)\right)\\ &\times q(\{\vec{r}''_n\},t|t_0). \end{aligned} \tag{3.36}$$

Again, in the limit as $t'\to t^+$ we find that

$$\begin{aligned}\frac{\partial}{\partial r''_{\alpha,m}}\left(\int\prod_n\{d\vec{r}_n\}q(\{\vec{r}_n\},t|\{\vec{r}''_n\},t)\right) &= \frac{\partial}{\partial r''_{\alpha,m}}\left(\int\prod_n\{d\vec{r}_n\delta(\vec{r}_n-\vec{r}''_n)\}\right)\\ &= \frac{\partial}{\partial r''_{\alpha,m}}\Big(1\Big)\\ &= 0. \end{aligned} \tag{3.37}$$

Thus $\boldsymbol{\phi}(\vec{r},t)=\vec{0}$ everywhere. An immediate result of this is that, from Eq. 3.14, $\omega(\vec{r},t)=0$ also. There are now just two mean-field equations:

$$\rho(\vec{r},t) = \frac{n_P}{Q([\boldsymbol{\psi}],t|t_0)}\sum_n q(\vec{r},n,t|t_0) \tag{3.38}$$

$$\psi_\alpha(\vec{r},t) = \frac{1}{\zeta_0}F_{ext,\alpha}(\vec{r})+\frac{1}{\zeta_0}\int d\vec{r}'\,\rho(\vec{r}',t)F_{int,\alpha}(\vec{r},\vec{r}'), \tag{3.39}$$

and since $\omega(\vec{r},t)=0$ everywhere, the modified functional Fokker-Planck equation Eq. 3.5 becomes simply the functional Fokker-Planck equation

$$\begin{aligned}\frac{\partial q(\{\vec{r}_n\},t|t_0)}{\partial t} &= \frac{k_BT}{\zeta_0}\sum_n\nabla^2_{\vec{r}_n}q(\{\vec{r}_n\},t|t_0)\\ &- \sum_n\nabla_{\vec{r}_n}\cdot\left[\left(\frac{1}{\zeta_0}\vec{F}_n(t)+\boldsymbol{\psi}(\vec{r}_n,t)\right)q(\{\vec{r}_n\},t|t_0)\right]. \end{aligned} \tag{3.40}$$

The prescription for the dynamical self-consistent field theory of polymers is contained in Eqs. 3.38, 3.39 and 3.40. We have intuitive physical interpretations for $\rho(\vec{r},t)$

(the time-dependent density field) and $\boldsymbol{\psi}(\vec{r},t)$ (the mean force field). The solution to these equations would be obtained self-consistently via a numerical algorithm. By guessing $\boldsymbol{\psi}$ for all space and time, $q(\vec{r},n,t|t_0)$ and $Q([\boldsymbol{\psi}],t|t_0)$ can in principle be calculated using Eq. 3.40. ρ followed by $\boldsymbol{\psi}$ can then be calculated via Eqs. 3.38 and 3.39 and the result for $\boldsymbol{\psi}$ compared to the initial guess. If the guessed $\boldsymbol{\psi}$ and calculated $\boldsymbol{\psi}$ differ, the guess is updated in the direction of the calculated $\boldsymbol{\psi}$ and the process is repeated until it converges and the difference between the guessed and calculated $\boldsymbol{\psi}$ is below a desired tolerance. This is a process analogous, once again, to what is done in equilibrium self-consistent field theory. A method for solving Eq. 3.40 efficiently, for a polymer with N connected beads described by the conformation $\{\vec{r}_n\}$, remains to be developed. However, by solving Eq. 3.40 for $q(\{\vec{r}_n\},t|t_0)$, we calculate *too much* information. All that we require in order to solve the mean-field equations is $q(\vec{r},n,t|t_0)$; it may be possible to obtain a method of calculating $q(\vec{r},n,t|t_0)$ efficiently by manipulating Eq. 3.40 in order to produce an evolution equation for $q(\vec{r},n,t|t_0)$, but this is beyond the scope of this thesis and will be dealt with in future work. The next chapter will focus on establishing, in a simple test case of interacting Brownian particles, that the iterative process of solving the mean-field equations self-consistently will work and that the theory produces physically sensible results.

Chapter 4

Test application of the theory

Having developed the complete dynamical self-consistent field theory in the previous chapter, it is important to next establish that the formalism works in a specific case, and gives physically sensible results. In particular, the mean-field equations and the modified Fokker-Planck equation (Eqs. 3.38, 3.39 and 3.40) need to be solved self-consistently in a process analogous to what is done in equilibrium self-consistent field theory. To do this we must

i) guess the mean force ψ for all space *and* all time (in contrast with equilibrium self-consistent field theory, where the field is guessed only for all space),

ii) calculate $q(\vec{r}, n, t|t_0)$ via the modified Fokker-Planck equation (Eq. 3.40),

iii) calculate $Q([\psi], t|t_0)$ and $\rho(\vec{r}, t)$ from $q(\vec{r}, n, t|t_0)$ using Eqs. 3.32 and 3.38,

iv) calculate $\psi(\vec{r}, t)$ from $\rho(\vec{r}, t)$ using Eq. 3.39,

v) compare the initial guess for ψ (ψ_{old}) to the calculated ψ (ψ_{calc}), and

vi) if they differ by more than 1×10^{-6} for any $(\vec{r}, t)$, update the guess for $\psi(\vec{r}, t)$: $\psi_{new}(\vec{r}, t) = \psi_{old}(\vec{r}, t) + \lambda(\psi_{calc}(\vec{r}, t) - \psi_{old}(\vec{r}, t))$ for some λ (the studies of this chapter used various values of λ ranging from 0.08 to 0.2), and go back to step ii).

vii) if they differ by less than 1×10^{-6} for *all* $(\vec{r}, t)$, the convergence process is complete.

Although such an approach has been shown to work for equilibrium self-consistent field theory, it is not clear as to whether obtaining a solution to the *dynamical* mean-field equations in this way will work. The essential difference in the dynamical case is that we must guess the mean field not only for all space, but also for all time. The procedure may not converge if the guess is inappropriate, so having to guess for all time is an additional complication. Also, the details of the equations are different from equilibrium self-consistent field theory: the mean-field equations involve forces rather than potentials, and a Fokker-Planck equation must be solved rather than a modified diffusion equation. With this in mind, this chapter will demonstrate that the self-consistency process works, in an application of the formalism to the problem of n_P Brownian particles in one dimension, interacting with each other via short-range repulsion in a harmonic trap, Figure 4.1. The choice of a harmonic potential is

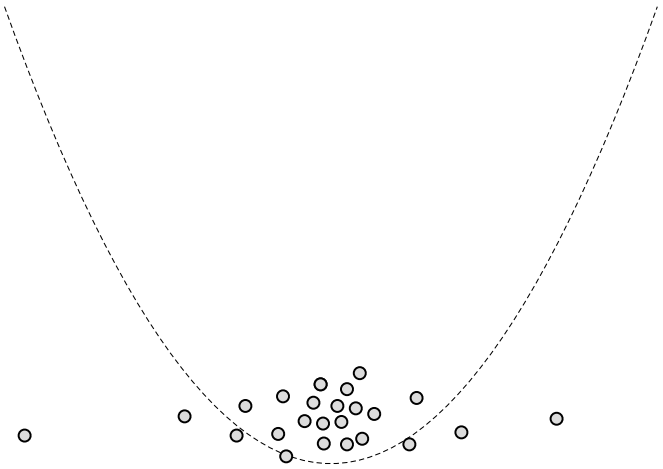

Figure 4.1: Brownian particles (grey circles) in a one-dimensional harmonic trap (dashed line).

primarily motivated by the polymer problem, which we will tackle in future work, in which there is a spring force between beads, but it may also be relevant to the problem of colloids caught in an optical trap. We will be interested in how quantities such as the center of mass and the width of the density profile are affected by changes in the strength of repulsion between particles. The mean-field equations for this problem may be derived from Eqs. 3.38, 3.39 and 3.40. There is no longer any n dependence in the theory or spring force between particles. Note that in this case, $q(\vec{r}, n, t|t_0)$ and $q(\{\vec{r}_n\}, t|t_0)$ become the same quantity, $q(\vec{r}, t|t_0)$.

4.1 Mean-field equations in one dimension

The mean-field equations in one dimension become

$$\rho(x,t) = \frac{n_P}{Q([\psi], t|t_0)} q(x, t|t_0) \tag{4.1}$$

$$\psi(x,t) = \frac{1}{\zeta_0} F_{ext}(x) + \frac{1}{\zeta_0} \int dx' \, \rho(x', t) F_{int}(x, x'), \tag{4.2}$$

where n_P is the number of particles, and the Fokker-Planck equation becomes

$$\frac{\partial q(x, t|t_0)}{\partial t} = \frac{k_B T}{\zeta_0} \frac{\partial^2 q(x, t|t_0)}{\partial x^2} - \frac{\partial}{\partial x} \left[\psi(x,t) q(x, t|t_0) \right]. \tag{4.3}$$

The harmonic potential is

$$U_{ext}(x) = \frac{1}{2} k x^2, \tag{4.4}$$

therefore $F_{ext}(x)$ is given by

$$F_{ext}(x) = -kx. \tag{4.5}$$

$F_{int}(x,x')$ is the short-range repulsive force on the particle at x due to the particle at x', and has the general form

$$F_{int}(x,x') = \sqrt{\frac{\pi}{2}}\epsilon F(X)\frac{X}{|X|} \tag{4.6}$$

where $X = x - x'$ and ϵ characterizes the strength of the repulsion. $F(X)$ is a symmetric function of narrow width, peaked at $X = 0$. A Gaussian form for $F(X)$ is convenient for the subsequent calculations:

$$F(X) = \sqrt{\frac{1}{2\pi l^2}}e^{-X^2/2l^2}, \tag{4.7}$$

where l characterizes the (short) range of the repulsion. Recalling Eq. 4.2 and the fact that $F_{int}(x,x')$ is short-ranged, we may Taylor expand $\rho(x',t)$ about $x' = x$:

$$\rho(x',t) = \rho(x,t) - \frac{\partial\rho(x,t)}{\partial x}X + \frac{1}{2}\frac{\partial^2\rho(x,t)}{\partial x^2}X^2 + \ldots \tag{4.8}$$

The integral in Eq. (4.2) may be evaluated:

$$\begin{aligned}\frac{1}{\zeta_0}\int dx'\rho(x',t)F_{int}(x,x') &= \sqrt{\frac{\pi}{2}}\frac{\epsilon}{\zeta_0}\int dX F(X)\left(\frac{X}{|X|}\rho(x,t) - \frac{X^2}{|X|}\frac{\partial\rho(x,t)}{\partial x}\right.\\ &+ \left.\frac{X^3}{2|X|}\frac{\partial^2\rho(x,t)}{\partial x^2} + \ldots\right).\end{aligned} \tag{4.9}$$

The first and third terms in the integral are zero since $F(X)$ is even. The second term may be evaluated to give

$$-\sqrt{\frac{\pi}{2}}\frac{\epsilon}{\zeta_0}\frac{\partial\rho(x,t)}{\partial x}\int dX\frac{X^2}{|X|}F(X) = -\sqrt{\frac{\pi}{2}}\frac{\epsilon}{\zeta_0}\int dX|X|F(X) = -\frac{\epsilon l}{\zeta_0}\frac{\partial\rho(x,t)}{\partial x}, \tag{4.10}$$

therefore

$$\psi(x,t) = -\frac{kx}{\zeta_0} - \frac{\epsilon l}{\zeta_0}\frac{\partial\rho(x,t)}{\partial x}. \tag{4.11}$$

The second term makes physical sense, as the repulsive force should push particles away from regions of high density. $\psi(x,t)$ can be written in the following form

$$\psi(x,t) = -\frac{kx}{\zeta_0} + \Psi(x,t) \tag{4.12}$$

which defines $\Psi(x,t)$. $\Psi(x,t)$ is a convenient choice because it is the quantity that we must guess in the first step of the self-consistent solution method and refine through iteration. The mean-field equations, then, are

$$\rho(x,t) = n_P \frac{q(x,t|t_0)}{Q([\Psi],t|t_0)} \tag{4.13}$$

$$\Psi(x,t) = -\frac{\epsilon l}{\zeta_0}\frac{\partial \rho(x,t)}{\partial x} \tag{4.14}$$

and the Fokker-Planck equation is

$$\frac{\partial q(x,t|t_0)}{\partial t} = \frac{k_B T}{\zeta_0}\frac{\partial^2 q(x,t|t_0)}{\partial x^2} + \frac{\partial}{\partial x}\left[\left(\frac{kx}{\zeta_0} - \Psi(x,t)\right) q(x,t|t_0)\right]. \tag{4.15}$$

For the purposes of solving these equations numerically, their dimensionless forms will be used. The length scale l_0 and the time scale τ associated with this problem can be identified as follows:

$$l_0^2 = \frac{2k_B T}{k} \tag{4.16}$$

and

$$\tau = \frac{\zeta_0}{k}. \tag{4.17}$$

We see that the relevant length scale is the one for which the energy of the harmonic potential is equal to $k_B T$, and the relevant time scale is given by the ratio of the friction coefficient to the spring constant. We may estimate what the length and time scales would be for a real Brownian particle in water, in an optical trap at room

temperature, for example. For a spherical particle of radius a in a solvent of viscosity η_s, the friction coefficient may be calculated [1] via

$$\zeta_0 = 6\pi\eta_s a. \tag{4.18}$$

For a particle of radius $a \sim 10^{-7}\ m$, where the viscosity of water at $T = 293K$ is $\eta_s = 10^{-3}\ Pa\cdot s$ [34], from Eq. 4.18 we have $\zeta_0 \sim 2\times 10^{-9}\ kg/s$. Estimating the spring constant for an optical trap as $k \sim 10^{-6}\ N/m$ [35, 36], we can calculate the length and time scales from Eqs. 4.16 and 4.17 as $l_0 \sim 10^{-7}\ m$ and $\tau \sim 2\ ms$, respectively.

The dimensionless mean-field equations are

$$\bar{\rho}(\bar{x},\bar{t}) = n_P \frac{\bar{q}(\bar{x},\bar{t}|\bar{t}_0)}{Q([\bar{\Psi}],\bar{t}|\bar{t}_0)} \tag{4.19}$$

$$\bar{\Psi}(\bar{x},\bar{t}) = -\tilde{\epsilon}\frac{\partial\bar{\rho}(\bar{x},\bar{t})}{\partial\bar{x}}, \tag{4.20}$$

and the dimensionless Fokker-Planck equation is

$$\frac{\partial\bar{q}(\bar{x},\bar{t}|\bar{t}_0)}{\partial\bar{t}} = \frac{1}{2}\frac{\partial^2\bar{q}(\bar{x},\bar{t}|\bar{t}_0)}{\partial\bar{x}^2} + \frac{\partial}{\partial\bar{x}}\left[\left(\bar{x} - \bar{\Psi}(\bar{x},\bar{t})\right)\bar{q}(\bar{x},\bar{t}|\bar{t}_0)\right], \tag{4.21}$$

where $\tilde{\epsilon}$ is defined as

$$\tilde{\epsilon} = \frac{\bar{\epsilon}l}{2l_0}. \tag{4.22}$$

The definitions of the dimensionless quantities are as follows:

$$\Psi(\bar{x},\bar{t}) = l_0\bar{\Psi}(\bar{x},\bar{t})/\tau, \qquad \rho(\bar{x},\bar{t}) = \bar{\rho}(\bar{x},\bar{t})/l_0, \qquad \epsilon = k_BT\bar{\epsilon},$$
$$x = l_0\bar{x}, \qquad\qquad t = \tau\bar{t}.$$

For the sake of simplicity, the dimensionless variables (designated by the overbar) will henceforth be written without the overbar. The remainder of this chapter assumes

that this is understood.

4.2 The Crank-Nicolson method

The Fokker-Planck equation is solved using a Crank-Nicolson scheme. The main advantages of the Crank-Nicolson scheme over a more straightforward approach such as Euler's method is that it is unconditionally stable and second-order accurate in both space and time [37]. This means that one can discretize the system with larger values of Δt and still maintain stability. The Crank-Nicolson discretization of the Fokker-Planck equation is

$$\begin{aligned}\frac{q_i^{n+1}-q_i^n}{\Delta t} &= \frac{1}{4(\Delta x)^2}\left[(q_{i+1}^{n+1}-2q_i^{n+1}+q_{i-1}^{n+1})+(q_{i+1}^n-2q_i^n+q_{i-1}^n)\right] \\ &+ \frac{1}{4\Delta x}\Big[(x_{i+1}-\Psi_{i+1}^{n+1})q_{i+1}^{n+1}-(x_{i-1}-\Psi_{i-1}^{n+1})q_{i-1}^{n+1} \\ &+ (x_{i+1}-\Psi_{i+1}^n)q_{i+1}^n-(x_{i-1}-\Psi_{i-1}^n)q_{i-1}^n\Big], \end{aligned} \tag{4.23}$$

where i is an integer labelling the position ($0 \leq i \leq N$) and N is the grid size, n is an integer labelling the timestep ($0 \leq n < T$) and T is the total number of timesteps. The time t_i is $n\Delta t$ and the position x_i is $\Delta x(i - N/2)$, where the final time is $T\Delta t$ and the size of the system, L, is $N\Delta x$. Multiplying both sides by Δt and arranging terms evaluated at the n^{th} timestep on the right hand side, and terms evaluated at the $(n+1)^{th}$ timestep on the left hand side

$$\begin{aligned}(1+2r)q_i^{n+1} & & \\ -(r-u\Psi_{i+1}^{n+1}+ux_{i+1})q_{i+1}^{n+1} & & \\ -(r+u\Psi_{i-1}^{n+1}-ux_{i-1})q_{i-1}^{n+1} &= (r-u\Psi_{i+1}^n+ux_{i+1})q_{i+1}^n \\ &+ (r+u\Psi_{i-1}^n-ux_{i-1})q_{i-1}^n \\ &+ (1-2r)q_i^n \end{aligned} \tag{4.24}$$

where

$$r = \frac{\Delta t}{4(\Delta x)^2} \tag{4.25}$$

and

$$u = \frac{\Delta t}{4\Delta x}. \tag{4.26}$$

The problem can be rewritten as a matrix equation to be solved for q_i^{n+1}:

$$A_{ij}^{n+1} q_j^{n+1} = c_i^n \tag{4.27}$$

where c_i^n is the right-hand side of Eq. 4.24 and A_{ij}^{n+1} is the matrix

$$\begin{pmatrix} diag_0 & upper_0 & 0 & 0 & 0 \\ lower_1 & diag_1 & upper_1 & 0 & 0 \\ 0 & lower_2 & \ddots & \ddots & 0 \\ 0 & 0 & \ddots & diag_{N-2} & upper_{N-2} \\ 0 & 0 & 0 & lower_{N-1} & diag_{N-1} \end{pmatrix}$$

where diag, upper and lower are the coefficients from Eq. 4.24 given by

$$diag_i = 1 - 2r \tag{4.28}$$

for $0 \leq i \leq N-1$, and

$$\begin{aligned} upper_i &= -r + u\Psi_{i+1}^{n+1} - ux_{i+1} \\ lower_i &= -r - u\Psi_{i-1}^{n+1} + ux_{i-1} \end{aligned} \tag{4.29}$$

for $1 \leq i \leq N-2$. The boundary conditions appear in the matrix as

$$\begin{aligned} upper_0 &= -2r \\ lower_0 &= 0 \\ upper_{N-1} &= 0 \\ lower_{N-1} &= -2r. \end{aligned} \tag{4.30}$$

Zero derivative and zero value boundary conditions are enforced on q_i^n:

$$q_0^n = q_{N-1}^n = 0 \tag{4.31}$$

and

$$\begin{aligned} q_{-1}^n &= q_1^n \\ q_{N-2}^n &= q_N^n \end{aligned} \tag{4.32}$$

as well as on ρ_i^n and Ψ_i^n. Eq. 4.27 may be solved efficiently, in $O(N)$ operations for each timestep [37], using a standard tridiagonal matrix solving algorithm.

4.3 Results

4.3.1 Non-interacting Brownian particles in a harmonic trap

We will examine the non-interacting case of 10 particles ($n_P = 10$) in a harmonic trap. The system length is 40 and the initial probability distribution is chosen to be Gaussian, centered on $x = -10$ with a width defined by $\sigma_0 = 0.5$. All of the results presented here use the lattice length $N = 800$ with $\Delta x = 0.05$ and $\Delta t = 0.0015625$. This way the results do not change to the sixth decimal place when

either Δx or Δt is decreased. The first task is to establish that numerical accuracy is being obtained. Although the Crank-Nicolson approach is stable for all Δx and Δt, it is not necessarily *accurate* for all Δx and Δt. The non-interacting case is useful for several reasons. First of all, since $\epsilon = 0$, $\Psi(x,t) = 0$ and so the self-consistent aspect of the problem is gone, making it simply a matter of solving the Fokker-Planck equation and then calculating $\rho(x,t)$. Secondly, it provides a means to establish numerical accuracy since the problem of non-interacting Brownian particles in a harmonic trap is exactly solvable [1]. Figure 4.2 shows the time evolution of

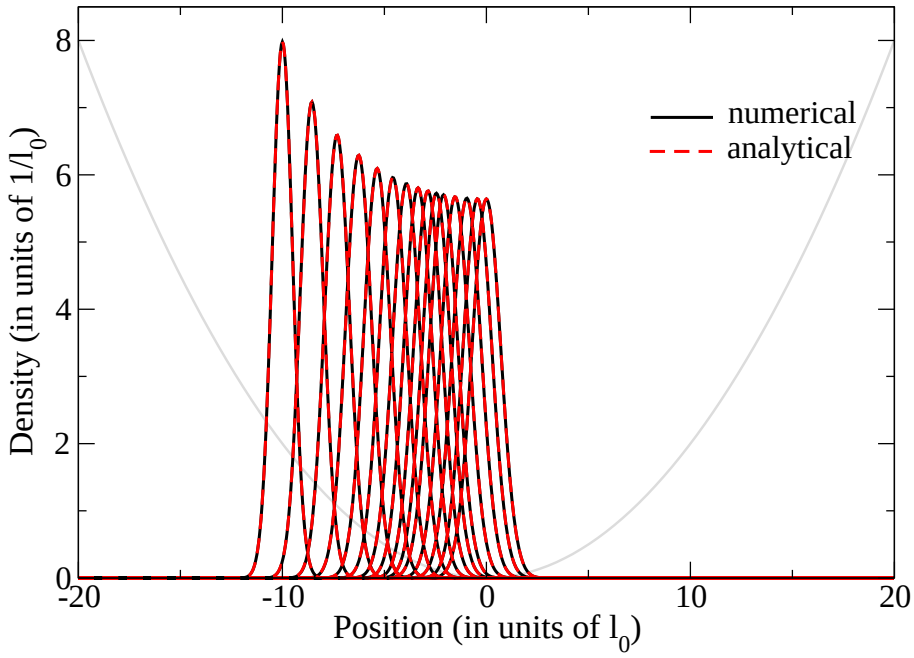

Figure 4.2: A comparison of the numerically-calculated time-dependent density distribution (black) to the analytical result (red dotted) [1], for a selection of times from $t = 0$ to $t = 9.984$, where equilibrium has been reached. The harmonic potential is shown in grey.

the density profile, where the densities at several different times have been overlaid to demonstrate the time evolution. The system evolves from its initial Gaussian

distribution, and has effectively reached the equilibrium distribution by $t = 10$. The spreading of the equilibrium distribution, as compared with the initial distribution, is a result of the competing effects of the harmonic potential (pushing the particles together) and thermal fluctuations (having the tendency to spread the particles out). Figure 4.2 also shows the comparison of the calculated distribution to the analytical result [1], which in terms of the dimensionless variables is given by

$$\rho(x,t) = \frac{n_P}{\sqrt{\pi\left(1+(2\sigma_0^2-1)e^{-2t}\right)}} \exp\left[\frac{-\left(x-x_0e^{-t}\right)^2}{\left(1+(2\sigma_0^2-1)e^{-2t}\right)}\right]. \tag{4.33}$$

The center-of-mass of the system may be tracked and also compared to the analytical result, which in terms of the dimensionless variables is given by

$$x_{CM}(t) = x_0e^{-t}. \tag{4.34}$$

Figure 4.3 is a plot of the calculated center-of-mass position as a function of time as well as the analytical result from Eq. 4.34. Since the Fokker-Planck equation is being solved via a finite-difference method, the fact that the agreement between numerical and analytical solutions is very good, as illustrated by Figures 4.2 and 4.3, indicates that our numerics are working properly and generating accurate results.

4.3.2 Interacting Brownian particles in a harmonic trap

Now that numerical accuracy has been established, the more interesting case of interacting Brownian particles may be examined. Note that the self-consistent iteration procedure was not required in the non-interacting case since in Eq. 4.20, $\Psi(x,t) = 0$ for $\epsilon = 0$, so the interacting case provides the opportunity to demonstrate that the mean-field equations can be solved in this self-consistent way by guessing $\Psi(x,t)$ for all x and t and updating it with each iteration until convergence. Figure 4.4 shows an initial guess for $\Psi(x,t)$ along with the converged form and an intermediate form

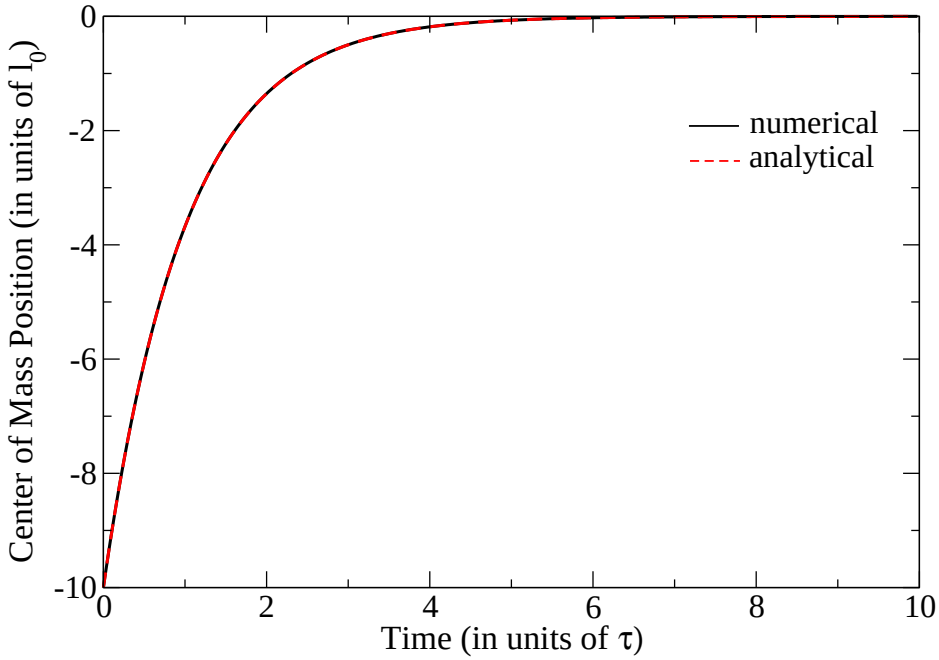

Figure 4.3: Center-of-mass position of the particle distribution function versus time, starting from a Gaussian centred at $x = -10$. The particles do not interact ($\epsilon = 0$). The solid black curve is the numerical result and the dashed red curve is the exact analytical result from Eq. 4.33. Interacting cases ($\epsilon \neq 0$) also exhibit the same center-of-mass motion.

(partway through the iteration process) for the $n_P = 10$ and $\epsilon = 1$ case. Figure 4.5

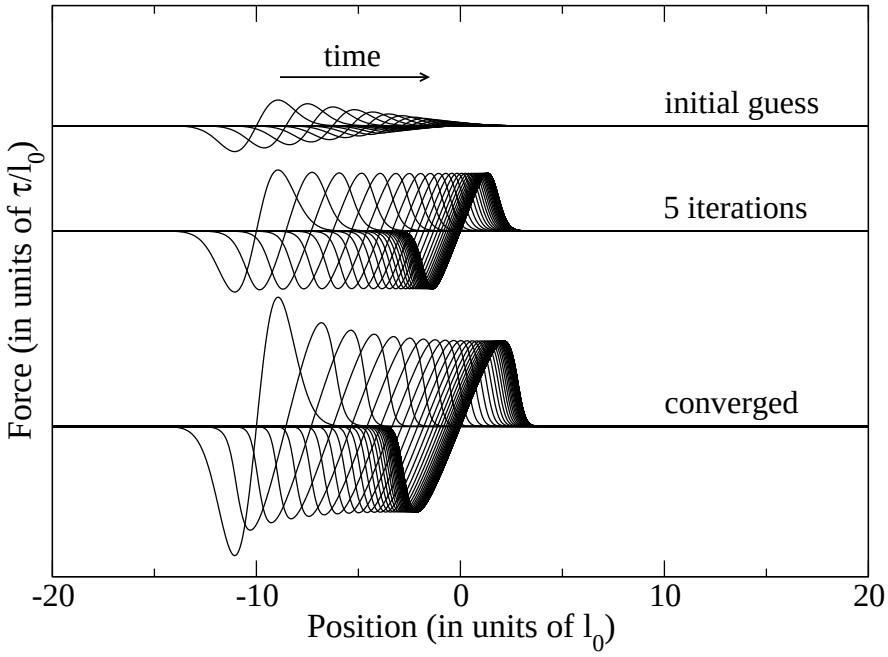

Figure 4.4: $\Psi(x,t)$ at various stages of the iteration process (top: initial guess; middle: intermediate, after 5 iterations; bottom: converged, after 218 iterations), for the $n_P = 10$ and $\epsilon = 1$ case.

shows the density profile for this case. The center-of-mass position versus time for the interacting case behaves exactly the same as the non-interacting case (Figure 4.3). This makes physical sense, since the repulsive interactions between particles are internal to the system and thus have no effect on the center-of-mass motion.

The spreading of the density distribution becomes more pronounced when the interaction strength ϵ is increased. We may examine the widths of the density profiles as a function of interaction strength, by defining the width $\sigma(t)$:

$$\sigma(t)^2 = \int dx \, (x - x_{CM}(t))^2 \, \frac{q(x,t|t_0)}{Q(t|t_0)}, \tag{4.35}$$

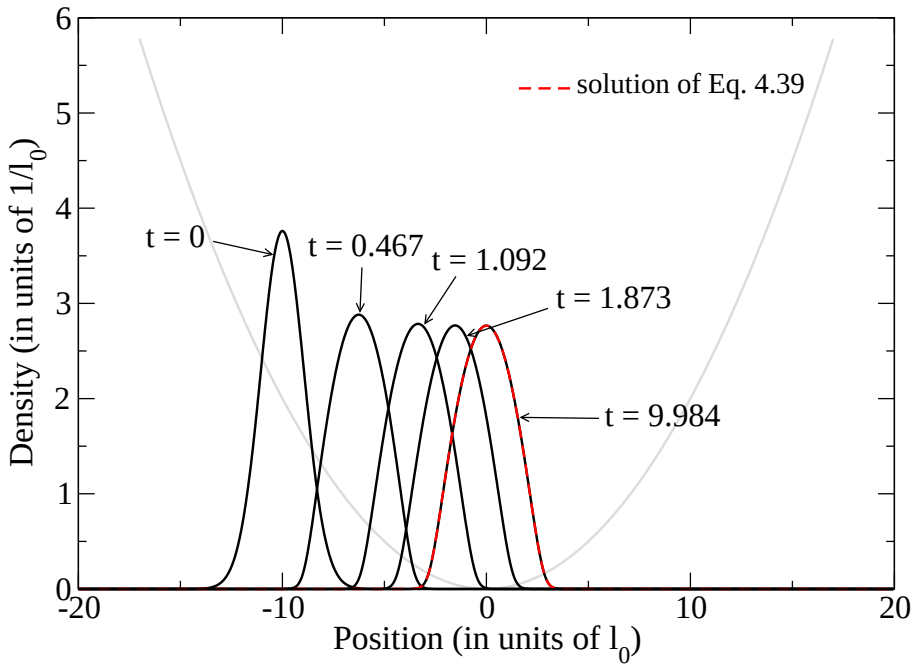

Figure 4.5: Density profiles for $t = 0, 0.467, 1.092, 1.873, 2.811$ and 9.984. $n_P = 10$ and $\epsilon = 1$. The harmonic potential is shown in grey. The red dashed curve is the numerical solution to Equation 4.39.

where the results shown here use an initial width given by $\sigma(0)^2 = 1.125$. Figure 4.6

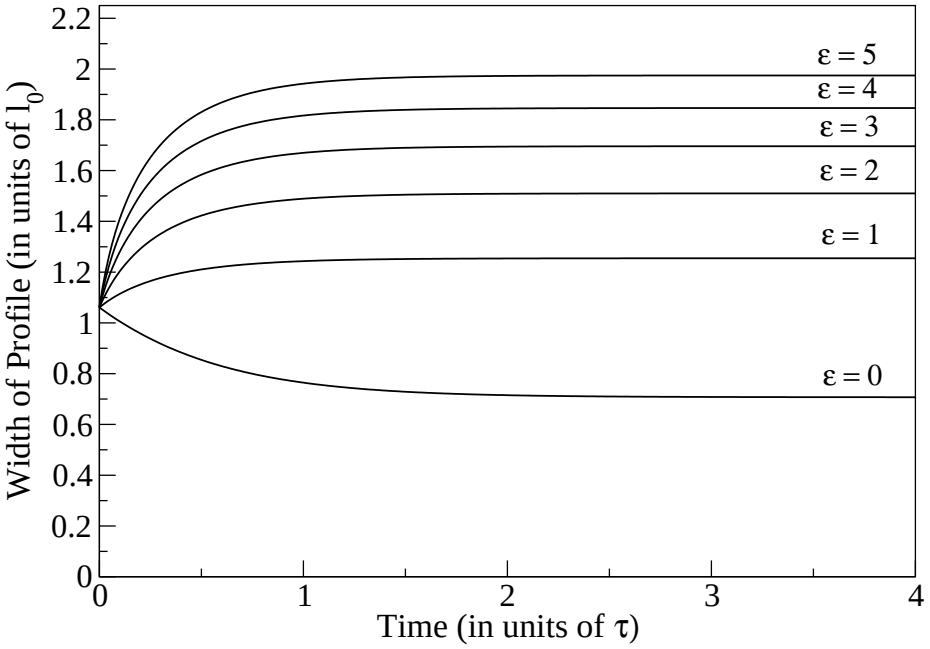

Figure 4.6: Density profile widths as a function of time for $n_P = 10$ and $\epsilon = 0$, 1, 2, 3, 4, 5.

shows the width of the density profiles as a function of time for different interaction strengths ϵ. Here we see the effect of turning on the repulsive interaction between particles: an increase in repulsion strength results in increased spreading of the density profiles, while the noninteracting case actually becomes more narrow (since the initial distribution was broader than the non-interacting equilibrium distribution). Note that each width approaches a constant, as equilibrium sets in at late times.

We may solve the Fokker-Planck equation for the equilibrium distribution in the mean-field interacting case. Substituting the mean-field equations for $\rho(x,t)$ and $\Psi(x,t)$ (Equations 4.19 and 4.20) into the Fokker-Planck equation (Equation 4.21)

and setting $\partial\rho(x,t)/\partial t = 0$:

$$0 = \frac{1}{2}\frac{d^2\rho(x)}{dx^2} + \frac{d}{dx}\left[\left(x + \epsilon\frac{d\rho(x)}{dx}\right)\rho(x)\right]. \tag{4.36}$$

Integrating both sides over x, we have

$$C_1 = \frac{1}{2}\frac{d\rho(x)}{dx} + \left(x + \epsilon\frac{d\rho(x)}{dx}\right)\rho(x). \tag{4.37}$$

The constant of integration C_1 is zero, since $\rho(x)$ and $d\rho(x)/dx$ approach zero as $x \to \pm\infty$ (provided that $\rho(x)$ approaches zero faster than $1/x$). By rearranging terms in Equation 4.37, we have

$$-\frac{1}{2\rho(x)}d\rho - \epsilon d\rho = x dx, \tag{4.38}$$

which may be integrated to give

$$-\frac{1}{2}\ln\rho(x) - \epsilon\rho(x) = \frac{1}{2}x^2 + C_2. \tag{4.39}$$

The integration constant C_2 may be determined numerically by requiring that the solution to Equation 4.39 conserves particle number and thus that $\rho(x)$ is appropriately normalized. The solution to Equation 4.39 for the $\epsilon = 1$ and $n_P = 10$ case is overlaid on Figure 4.5. The agreement is excellent. If we multiply both sides of Equation 4.39 by $\rho(x)$ and reintroduce the correct non-dimensionless pre-factors (from Equations 4.13, 4.14 and 4.15) we have

$$-k_BT\rho(x)\ln\rho(x) - \epsilon l\rho(x)^2 = \frac{1}{2}kx^2\rho(x) + C_2\rho(x), \tag{4.40}$$

which provides expressions for the entropy ($k_BT\rho\ln\rho$) as well as the energies of the repulsive ($\epsilon l\rho$) and harmonic potential ($\frac{1}{2}kx^2\rho$) interactions. The free energy of

equilibrium states in this single-species interacting problem is thus accessible to us.

It is a non-trivial result that a self-consistent solution that makes physical sense can be found for this interacting problem. This helps to confirm our confidence in the novel technique we have developed. We may, however, investigate further properties of systems of interacting Brownian particles. For example, we would expect the center-of-mass motion to be ϵ-dependent if two localized particle distributions were initialized on opposite ends of the harmonic potential minimum, since one distribution can exert a force on the other. We may examine such a 'binary system' with particle types A and B, where the strengths of interaction between like and unlike particles are not necessarily the same.

In the non-interacting case, each localized particle distribution moves independently of the other and there is no perturbation to the center-of-mass motion from Figure 4.3. In the interacting case, when the two distributions become close enough to feel the repulsion, the center-of-mass motion of each individual distribution should be slowed down relative to the non-interacting and single-distribution case.

4.3.3 Binary system of interacting Brownian particles in a harmonic trap

The formalism is generalized to describe a binary system with type A and type B particles in Appendix B.6. There are three interaction strength parameters instead of one: ϵ_{AA}, the repulsion strength between type A particles, ϵ_{BB}, the repulsion strength between type B particles and ϵ_{AB}, the repulsion strength between type A and type B particles. When the difference between interaction strengths of like and unlike species is great enough, we expect to observe macrophase separation. Studying the kinetics of macrophase separation in such binary systems will help to inform future studies of microphase separation dynamics in block copolymer melts.

From Appendix B.6, the dimensionless mean-field equations are

$$\rho_A(x,t) = n_A \frac{q_A(x,t|t_0)}{Q_A(t|t_0)}, \tag{4.41}$$

$$\rho_B(x,t) = n_B \frac{q_B(x,t|t_0)}{Q_B(t|t_0)}, \tag{4.42}$$

$$\Psi_A(x,t) = -\frac{\epsilon_{AA} n_A}{Q_A(t|t_0)} \frac{\partial q_A(x,t|t_0)}{\partial x} - \frac{\epsilon_{AB} n_B}{Q_B(t|t_0)} \frac{\partial q_B(x,t|t_0)}{\partial x}, \tag{4.43}$$

$$\Psi_B(x,t) = -\frac{\epsilon_{BB} n_B}{Q_B(t|t_0)} \frac{\partial q_B(x,t|t_0)}{\partial x} - \frac{\epsilon_{AB} n_A}{Q_A(t|t_0)} \frac{\partial q_A(x,t|t_0)}{\partial x}, \tag{4.44}$$

and the dimensionless Fokker-Planck equations for $q_A(x,t|t_0)$ and $q_B(x,t|t_0)$

$$\frac{\partial q_A(x,t|t_0)}{\partial t} = \frac{1}{2} \frac{\partial^2 q_A(x,t|t_0)}{\partial x^2} + \frac{\partial}{\partial x} \left[(x - \Psi_A(x,t))\, q_A(x,t|t_0) \right], \tag{4.45}$$

$$\frac{\partial q_B(x,t|t_0)}{\partial t} = \frac{1}{2} \frac{\partial^2 q_B(x,t|t_0)}{\partial x^2} + \frac{\partial}{\partial x} \left[(x - \Psi_B(x,t))\, q_B(x,t|t_0) \right]. \tag{4.46}$$

where $q_A(x,t|t_0)$ is the propagator for species A and $q_B(x,t|t_0)$ is the propagator for species B. We may define a useful quantity χ that characterizes the difference in interaction strengths between like and unlike particles:

$$\chi = \epsilon_{AB} - \frac{1}{2} (\epsilon_{AA} + \epsilon_{BB}). \tag{4.47}$$

Figure 4.7 shows the time evolution of the density profile of two localized particle distributions of types A and B ($n_A = n_B = 5$) with $\chi = 0$. In this case the type A and type B particles are physically identical, as $\epsilon_{AA} = \epsilon_{BB} = \epsilon_{AB} = 0.50$ (ie. A and B are only labels). At approximately $t = 2$, the two distributions begin interacting with each other. Their motion is visibly slowed and each distribution is squeezed by the repulsion of the other particles on one side and the harmonic potential on the other. The narrow shape of the resulting distributions at, for example, $t = 2.811$ reflects this. At late times, equilibrium sets in (beginning at approximately $t = 12$) and

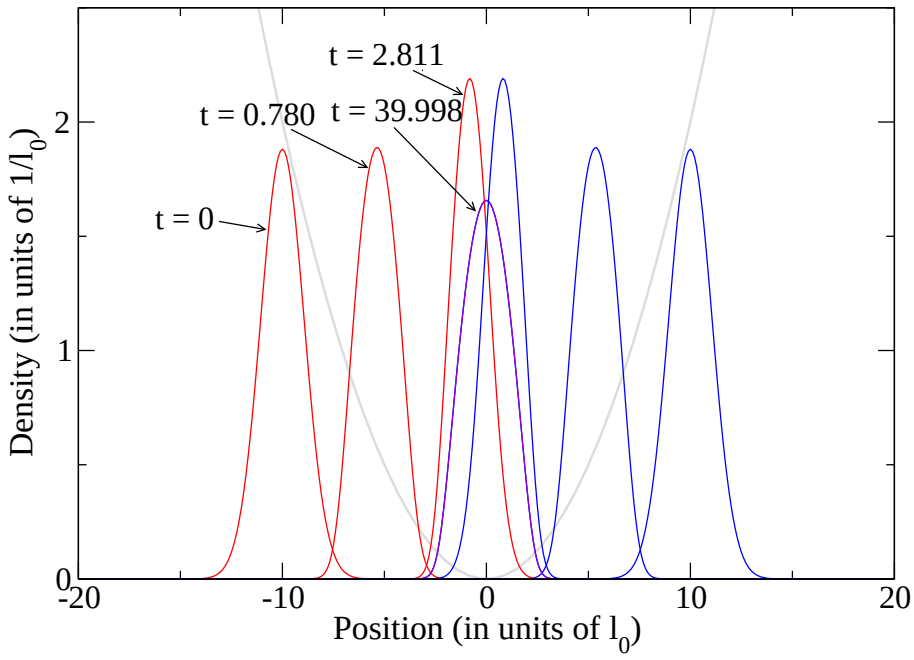

Figure 4.7: Density profiles for Type A (red) and Type B (blue) particles as a function of time. $n_A = 5$, $n_B = 5$, $\epsilon_{AA} = \epsilon_{BB} = \epsilon_{AB} = 0.50$ and $\chi = 0$. $t = 0$, 0.780, 2.811, 39.998. The harmonic potential is shown in grey.

the two localized particle distributions have completely mixed. The sum of the two distributions gives the same behaviour as if we were to examine the same system using the single-species formalism with $\epsilon = 0.50$, where we do not label the two localized distributions differently.

The center-of-mass motion will be slowed once the localized particle distributions begin interacting at around $t = 2$. We may examine the center-of-mass trajectory of the localized particle type B distribution as a function of χ, shown in Figure 4.8. The

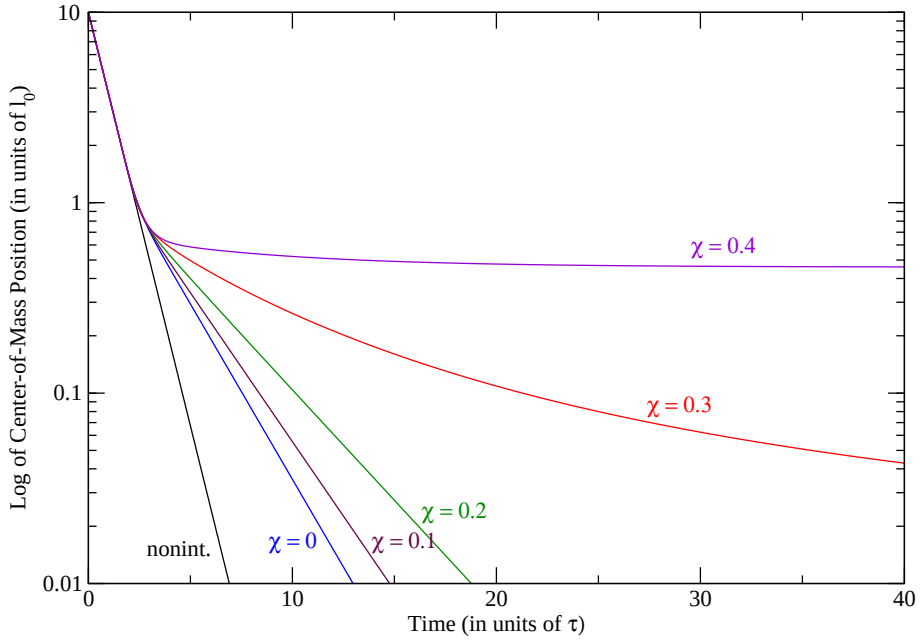

Figure 4.8: Center-of-mass position versus time for type B particles colliding with type A particles, on a semi-log graph. $n_A = 5$, $n_B = 5$, for the non-interacting case (black), where $\epsilon_{AA} = \epsilon_{BB} = \epsilon_{AB} = \chi = 0$ as well as interacting cases with $\epsilon_{AB} = 0.50$, $\epsilon_{AA} = \epsilon_{BB}$ and $\chi = 0$ (blue), 0.1 (maroon), 0.2 (green), 0.3 (red) and 0.4 (violet). Deviation from the black curve, beginning around $t = 2$, shows the influence of repulsive forces from the A particles on the center-of-mass motion of the B distribution. The blue, maroon and green curves decay exponentially until the collision, and after the collision decay exponentially but with a different decay time. The violet curve ($\chi = 0.4$) approaches some non-zero asymptote, indicating the onset of segregation in the system.

manner in which the center-of-mass motion is affected by the repulsive interaction between particles depends on the magnitudes of the ϵ parameters, even if two sets of ϵ parameters gives the same χ. Comparing the non-interacting case and the interacting case with $\chi = 0$ from Figure 4.8, we see a difference in the center-of-mass trajectories despite the fact that both cases have $\chi = 0$, so clearly the kinetics of the process depends ultimately on the magnitudes of the ϵ parameters and not on χ. There are two striking features in Figure 4.8. The $\chi = 0$, $\chi = 0.1$ and $\chi = 0.2$ curves decay exponentially until the collision, and decay exponentially again after the collision but with a different decay time. The other interesting feature is that for the $\chi = 0.40$ case, the center-of-mass position for the type A particle does not asymptotically approach zero; rather, it approaches some non-zero asymptote. This indicates that the effective affinity of like particles in this case is great enough in comparison to that of unlike particles that the system remains segregated. We expect that there is some transition defining the onset of segregation, which occurs for χ somewhere between 0.30 and 0.40.

This behaviour may be investigated further; Figure 4.9 shows some late-time ($t = 39.998$) density profiles for types A and B particles with $\epsilon_{AB} = 0.50$ and $\chi = 0.20$, 0.30 and 0.40. Type A particles were initialized as two localized particle distributions centered on $x = -10$ and $x = 10$ and type B was initialized in the center, as shown at the top of Figure 4.9. The $\chi = 0.20$ case has reached equilibrium (the density profiles are no longer changing), and the species A and B have become completely mixed. The $\chi = 0.40$ case has also reached equilibrium but in this case the two species remain segregated, as we expect from Figure 4.8. The $\chi = 0.30$ case, intermediate between the other two, is still in the process of becoming fully mixed at $t = 39.998$. We find that as we get closer to the suspected transition point, the system takes longer to equilibrate; it therefore becomes difficult to accurately identify the transition, since we cannot tell if the system will be in a mixed or segregated equilibrium state until it

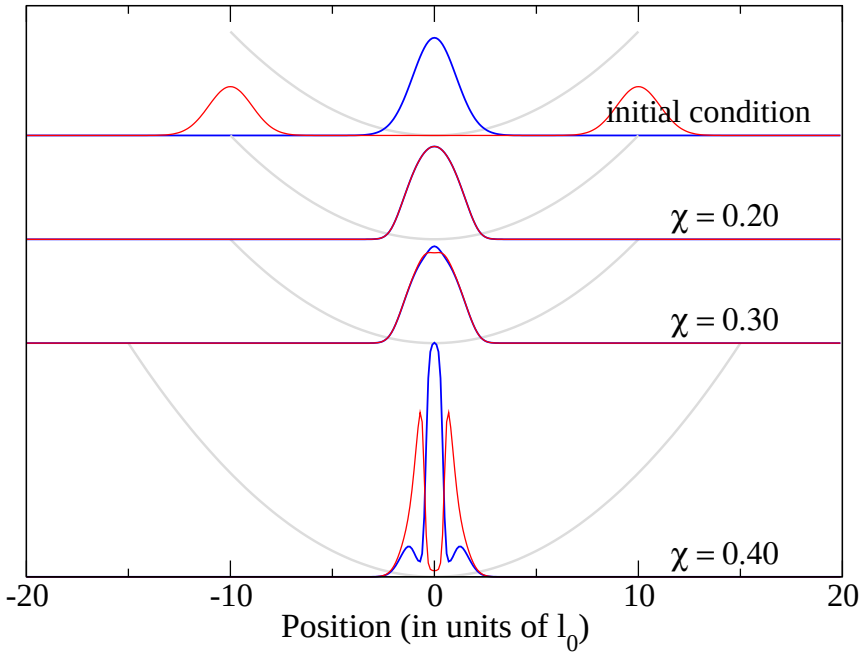

Figure 4.9: Type A (red) and type B (blue) density profiles at t = 39.998, for the three cases $\chi = 0.20$, 0.30 and 0.40, with $\epsilon_{AB} = 0.50$, $\epsilon_{AA} = \epsilon_{BB}$ and $n_A = 5$, $n_B = 5$. The initial condition for all three cases, and the harmonic potential (grey) is also shown.

has equilibrated. It may also be suspected that the equilibrium configuration of the $\chi = 0.4$ case is a meta-stable state; that the configuration where all of the type A particles are mixed instead of separated by the type B particles in the center would have lower surface free energy and therefore be the stable equilibrium state. However, the presence of the type B particles in the center presents a significant energy barrier that prevents this state from being accessed. In principle, the transition and stable states could be identified via equilibrium theory; it would be fruitful to perform a free energy calculation in combination with the analysis done here in order to determine the stable equilibrium state as a function of interaction strengths. However, this is beyond the scope of the thesis and will not be done here.

The results presented in this chapter were generated by code written in the C programming language and run on a laptop computer ($\sim$20 Gflops). A typical run of the code can be as short as a matter of seconds (in the non-interacting case) and as long as tens of minutes (in the interacting case). The most costly runs (in terms of time) were those used to generate the plots of Figure 4.9, for which it took several hours to obtain all of the necessary data. In terms of memory requirements, the code was not optimized in any way. For a one-dimensional system size of 800, run for approximately 10^4 timesteps on a binary system (doubling the number of arrays) and storing the data at all timesteps, the memory allocation requirements of the program are on the order of a gigabyte. This can be cut down significantly using various methods such as subdividing the total number of timesteps into a series of shorter runs (which could each be as short as a single timestep; this will *drastically* reduce memory requirements), or adaptive timestepping which procedurally modifies the length of each timestep, Δt, based on how quickly the system is evolving. In the two- or three-dimensional case, these optimization methods can help to maintain a memory allocation requirement on the order of gigabytes. We expect that a 3D system running an optimized code with reasonable parameters (a system size of 200^3,

for example) could run on a core cluster ($\sim 10^3$ Gflops) in approximately a day.

The results presented in this chapter, beyond simply demonstrating that the mean-field equations can indeed be solved (efficiently) by this self-consistent iterative process, have shown that the system possesses realistic physical properties under the dynamical mean-field approximation. We have generated some non-trivial results for the dynamics of single particles (both of a single species and for binary blends). Since this study was intended to simply test the method of self-consistently solving the mean-field equations, a more comprehensive study has not been performed at this point. The exercise nonetheless serves to establish the potential of applying the formalism to a scenario where the mean-field approximation might be suspected to be very good, such as a polymer melt in three dimensions.

Chapter 5

Conclusion

We produced a complete formalism for a dynamical self-consistent field theory of polymers. This work goes beyond that of Fredrickson and others [30, 31] in that we treat the single-chain dynamics exactly, and employ a dynamical saddle-point approximation which results in a set of dynamical mean-field equations with a clear physical interpretation in terms of the time-dependent density and mean force fields. The single-chain dynamics are treated exactly via a key quantity $q(\{\vec{r}_n\}, t|t_0)$ which satisfies a functional Fokker-Planck equation. The structure of the theory is similar to that of equilibrium self-consistent field theory, demonstrating that the theory we have developed is a natural dynamical analogue of equilibrium self-consistent field theory. The wealth of sophisticated solution techniques from equilibrium SCFT may be applied to it. It is fully flexible in terms of the number n_P and length N of polymers, the interaction between polymers $\vec{F}_{int}$ and the forces due to the external environment $\vec{F}_{ext}$. Important dynamical problems, which are the focus of much current research in polymer dynamics (such as electrophoresis, translocation and reptation), are thus accessible via the theory. The relationships between the parameters of the mean-field and Fokker-Planck equations and the microscopic model are also clearly defined, a feature not present in many other dynamical polymer field theories. In particular,

our timescale $\tau = \zeta_0/k$ is directly related to measurable microscopic quantities, like the monomeric friction constant. Thus, unlike many other dynamical polymer field theories, we know the real time scale in our theory.

We demonstrated that the mean-field equations can be solved self-consistently and that the results generated by the theory are physically reasonable. The theory was applied to the simple case of n_P interacting Brownian particles in a harmonic external potential in one dimension. The interaction between particles, a short-range repulsive interaction, introduced a non-trivial element to the problem and was shown to produce some interesting results such as broadening of the density profile and deflection of the center-of-mass trajectories of two colliding localized density distributions. A binary system of particle types A and B was shown to demonstrate segregation when the difference of interaction strengths between like and unlike particles was large enough. The kinetics of the collisions and subsequent mixing depends not only on the interaction strength difference parameter χ but on the magnitudes of the interaction strengths themselves.

Applying the theory to polymers presents a challenge for the reasons alluded to in Chapter 3 involving the efficiency of the current prescription for calculating the time-dependent density. This issue may be resolved by investigating methods of efficiently calculating the *required* quantity $q(\vec{r}, n, t|t_0)$ (proportional to the probability of finding the n^{th} monomer at position $\vec{r}$ at time t) by modifying the functional Fokker-Planck equation. The sophisticated techniques from equilibrium SCFT can also be drawn upon to tackle this challenge. With future work, we aim to resolve this issue and then apply the theory to the electrophoresis problem, with a polymer passing through an array of fixed periodic obstacles, where we expect to see a crossover to reptation for long chains. This "toy-model" for reptation will be useful in elucidating how confinement perpendicular to the chain backbone manifests itself in the dynamical behaviour. Then we can study reptation in melts, where the obstacles are other,

moving, polymers.

Appendix A

Analogy with equilibrium self-consistent field theory

This Appendix is intended to briefly highlight the analogy between the formalism presented in this thesis (of *dynamical* self-consistent field theory) and that of equilibrium self-consistent field theory. The formalism presented here will be that of a binary blend of n_A homopolymers of type A of length N_A, and n_B homopolymers of type B of length N_B, and is based on the discussion and notation of Schmid [10].

The underlying model of this formalism is the continuous Gaussian chain, which is a continuum bead-spring model described by the Edwards Hamiltonian

$$\frac{H_G[\vec{R}(s)]}{k_BT} = \frac{3}{2b^2}\int_0^N ds \left(\frac{d\vec{R}(s)}{ds}\right)^2, \tag{A.1}$$

where the chain contour is described by $\vec{R}(s)$ and b is the statistical segment length (the spring force we use in the Rouse model (Eq. 2.2) may be derived from the discrete form of the Edwards Hamiltonian). The interaction between polymers is described

by a Flory-Huggins interaction term

$$\frac{H_I[\hat{\phi}_A, \hat{\phi}_B]}{k_B T} = \rho_0 \chi \int d\vec{r} \hat{\phi}_A \hat{\phi}_B \tag{A.2}$$

where $\hat{\phi}_j$ are 'monomer volume fractions' of polymers of type j

$$\hat{\phi}_j(\vec{r}) = \frac{1}{\rho_0} \sum_{\alpha=1}^{n_j} \int_0^{N_j} ds\, \delta(\vec{r} - \vec{R}_{j,\alpha}(s)), \tag{A.3}$$

where α labels the polymers, $\vec{R}_{j,\alpha}(s)$ is the position of the s^{th} monomer on the α^{th} polymer of type j, and χ is the Flory-Huggins parameter which contains the microscopic features of the blend and characterizes the incompatibility of the unlike monomer species in the blend. The canonical partition function is

$$Z = \frac{1}{n_A! n_B!} \left[\prod_\alpha \rho_0 \int D[\vec{R}_\alpha(s)] e^{-H_G[\vec{R}_\alpha(s)]/k_B T} \right] e^{-\rho_0 \chi \int d\vec{r} \hat{\phi}_A \hat{\phi}_B} \delta[\hat{\phi}_A + \hat{\phi}_B - 1] \tag{A.4}$$

where an incompressibility condition has also been imposed (that is, $\hat{\phi}_A + \hat{\phi}_B = 1$ everywhere). This partition function is analogous to the functional integral $Z(t|t_0)$ (Eq. 2.12) that appears in the dynamical SCFT.

Next, the path integrals in Z are decoupled by inserting delta functionals

$$1 = \int D[\phi_j] \delta[\phi_j - \hat{\phi}_j], \tag{A.5}$$

and using the Fourier-transform representations of the delta functionals

$$\delta[\phi_j - \hat{\phi}_j] = \int_{-i\infty}^{i\infty} D[W_j] \exp\left(\frac{\rho_0}{N} \int d\vec{r} W_j (\phi_j - \hat{\phi}_j) \right) \tag{A.6}$$

$$\delta[\phi_A + \phi_B - 1] = \int_{-i\infty}^{i\infty} D[\xi] \exp\left(\frac{\rho_0}{N} \int d\vec{r} \xi (\phi_A + \phi_B - 1) \right). \tag{A.7}$$

where N is some reference chain length, and is introduced for convenience. Z is

rewritten

$$Z \propto \int_{-i\infty}^{i\infty} D[W_A]D[W_B]D[\xi] \int_{-\infty}^{\infty} D[\phi_A]D[\phi_B]e^{-F/k_BT} \tag{A.8}$$

and F has the form

$$\begin{aligned} \frac{F[W_A, W_B, \xi, \phi_A, \phi_B]}{k_BT} &= \frac{\rho_0}{N}\left\{\int d\vec{r}\,(\chi N\phi_A\phi_B - W_A\phi_A - W_B\phi_B - \xi(\phi_A + \phi_B - 1)) \right. \\ &- \left. V_A\frac{N}{N_A}\ln\left(\rho_0\frac{Q_A}{n_A}\right) - V_B\frac{N}{N_B}\ln\left(\rho_0\frac{Q_B}{n_B}\right)\right\}, \end{aligned} \tag{A.9}$$

where Q_j is the single-chain partition function

$$Q_j = \int D[\vec{R}(s)]e^{-H_G[\vec{R}(s)]/k_BT}e^{-\frac{1}{N}\int_0^{N_j} ds\, W_j(\vec{R}(s))} \tag{A.10}$$

for $j = A, B$. The process of writing Z in terms of collective field variables and coarse-graining, culminating in Eqs. A.8, A.9 and A.10, is analogous to the developments of Chapter 2 and the resulting Eqs. 2.23, 2.24 and 2.27.

The mean-field approximation consists of replacing Z with its saddle point value, by minimizing F with respect to the field variables ϕ_j and W_j. The resulting mean-field equations are

$$\phi_A = \frac{n_A}{\rho_0 Q_A}\int_0^{N_A} ds\, q_A(\vec{r}, s)q_A^\dagger(\vec{r}, N-s) \tag{A.11}$$

$$\phi_B = \frac{n_B}{\rho_0 Q_B}\int_0^{N_B} ds\, q_B(\vec{r}, s)q_B^\dagger(\vec{r}, N-s) \tag{A.12}$$

$$W_A = \chi N\phi_B - \xi \tag{A.13}$$

$$W_B = \chi N\phi_A - \xi \tag{A.14}$$

where $q_j(\vec{r}, s)$ and $q_j^\dagger(\vec{r}, s)$ are propagators which satisfy the modified diffusion equa-

tions

$$\frac{\partial q_j(\vec{r},s)}{\partial s} = \left(\frac{b^2}{6}\nabla^2 - \frac{W_j(\vec{r},s)}{N}\right) q_j(\vec{r},s) \tag{A.15}$$

$$\frac{\partial q_j^\dagger(\vec{r},s)}{\partial s} = \left(\frac{b^2}{6}\nabla^2 - \frac{W_j(\vec{r},N-s)}{N}\right) q_j^\dagger(\vec{r},s) \tag{A.16}$$

and are related to Q_j by

$$Q_j = \int d\vec{r}\, q_j(\vec{r},N) = \int d\vec{r}\, q_j^\dagger(\vec{r},N). \tag{A.17}$$

Equations A.11-A.14, along with the incompressibility constraint $\phi_A+\phi_B = 1$, can be solved self-consistently by guessing W_j, solving the modified diffusion equations A.15-A.16 (using either a reciprocal-space basis function decomposition, a direct real-space approach, or an operator-splitting method combining real- and reciprocal-space techniques), calculating ϕ_j, re-calculating W_j and comparing the calculated W_j to the guessed W_j. The guess W_j is updated if the two are not the same (within some tolerance), and the process is iterated until it converges. The mean-field approximation to Z, the definition of the propagators and the self-consistent method for solving the mean-field equations are analogous, again, to the developments of Chapter 3.

Appendix B

Derivations and technical details

B.1 Averaging $Z_f(t|t_0)$ over the noise

We wish to calculate the noise-averaged functional integral $Z(t|t_0) = \langle Z_f(t|t_0)\rangle_f$. Before averaging, $Z_f(t|t_0)$ is given by

$$\begin{aligned} Z_f(t|t_0) &= \int \prod_l \left(\prod_n \{d\vec{R}_n^{(l)}(t_0)\} P_0(\{\vec{R}_n^{(l)}(t_0)\}) \right) \int \prod_{l,n} \left\{ D[\vec{R}_n^{(l)}(t')] D[\hat{\vec{R}}_n^{(l)}(t')] \right\} \\ &\times \exp\left[\sum_{l,n} \int_{t_0}^{t} dt'\, i\hat{\vec{R}}_n^{(l)}(t') \cdot \left(\frac{\partial \vec{R}_n^{(l)}(t')}{\partial t'} - \frac{1}{\zeta_0}\vec{F}_n^{(l)}(t') - \frac{1}{\zeta_0}\vec{F}_{ext}(\vec{R}_n^{(l)}(t')) \right.\right. \\ &- \left.\left. \frac{1}{\zeta_0} \sum_{l',m} \vec{F}_{int}(\vec{R}_n^{(l)}(t'), \vec{R}_m^{(l')}(t')) - \frac{1}{\zeta_0}\vec{f}_n^{(l)}(t') \right) \right]. \end{aligned} \tag{B.1}$$

$Z(t|t_0)$ is then given by

$$\begin{aligned} Z(t|t_0) &= \int \prod_{l,n} D[\vec{f}_n^{(l)}(t')] P[\vec{f}_n^{(l)}(t')] \int \prod_l \left(\prod_n \{ d\vec{R}_n^{(l)}(t_0) \} P_0(\{\vec{R}_n^{(l)}(t_0)\}) \right) \\ &\times \int \prod_{l,n} \left\{ D[\vec{R}_n^{(l)}(t')] D[\hat{\vec{R}}_n^{(l)}(t')] \right\} \exp \left[\sum_{l,n} \int_{t_0}^{t} dt' \, i\hat{\vec{R}}_n^{(l)}(t') \cdot \left(\frac{\partial \vec{R}_n^{(l)}(t')}{\partial t'} \right.\right. \\ &- \left.\left. \frac{1}{\zeta_0} \vec{F}_n^{(l)}(t') - \frac{1}{\zeta_0} \vec{F}_{ext}(\vec{R}_n^{(l)}(t')) - \frac{1}{\zeta_0} \sum_{l',m} \vec{F}_{int}(\vec{R}_n^{(l)}(t'), \vec{R}_m^{(l')}(t')) - \frac{1}{\zeta_0} \vec{f}_n^{(l)}(t') \right) \right], \end{aligned} \tag{B.2}$$

where $P[\vec{f}_n^{(l)}(t')]$ is the probability of the particular noise realization $\vec{f}_n^{(l)}(t')$ for all l, n and t'. Here, we assume that $P[\vec{f}_n^{(l)}(t')]$ is Gaussian-distributed and satisfies Eqs. 2.5 and 2.6:

$$P[\vec{f}_n^{(l)}(t')] = \frac{\exp\left(-\frac{1}{4\zeta_0 k_B T} \sum_{n,l} \int dt' \, \vec{f}_n^{(l)^2}(t') \right)}{\int D[\vec{f}_n^{(l)}(t')] \exp\left(-\frac{1}{4\zeta_0 k_B T} \sum_{l,n} \int dt' \, \vec{f}_n^{(l)^2}(t') \right)}, \tag{B.3}$$

such that

$$\left\langle f_{\alpha,n}^{(l)}(t) \right\rangle = 0 \tag{B.4}$$

and

$$\left\langle f_{\alpha,n}^{(l)}(t) f_{\beta,m}^{(l')}(t') \right\rangle = 2\zeta_0 k_B T \delta_{\alpha\beta} \delta_{ll'} \delta_{nm} \delta(t - t'). \tag{B.5}$$

To calculate $Z(t|t_0)$, then, we must calculate

$$\frac{\int D[\vec{f}_n^{(l)}(t')] \exp\left[-\sum_{l,n} \int dt' \left(\frac{i}{\zeta_0} \hat{\vec{R}}_n^{(l)}(t') \cdot \vec{f}_n^{(l)}(t') + \frac{1}{4\zeta_0 k_B T} f_n^{(l)^2}(t') \right) \right]}{\int D[\vec{f}_n^{(l)}(t')] \exp\left(-\frac{1}{4\zeta_0 k_B T} \sum_{l,n} \int dt' \, f_n^{(l)^2}(t') \right)}, \tag{B.6}$$

which may be decomposed into a product (over l, n and t') of integrals:

$$\prod_{l,n,t'} \frac{\int d\vec{f}_n^{(l)}(t') \exp\left(-\frac{i}{\zeta_0} \hat{\vec{R}}_n^{(l)}(t') \cdot \vec{f}_n^{(l)}(t') - \frac{1}{4\zeta_0 k_B T} f_n^{(l)^2}(t') \right)}{\int d\vec{f}_n^{(l)}(t') \exp\left(-\frac{1}{4\zeta_0 k_B T} f_n^{(l)^2}(t') \right)}. \tag{B.7}$$

These are standard Gaussian integrals, and the result is

$$\prod_{l,n,t'} \exp\left(-\frac{k_B T}{\zeta_0}\hat{R}_n^{(l)^2}(t')\right) = \exp\left(-\frac{k_B T}{\zeta_0}\sum_{l,n}\int dt'\, \hat{R}_n^{(l)^2}(t')\right). \tag{B.8}$$

We may therefore write $Z(t|t_0)$ as

$$\begin{aligned} Z(t|t_0) &= \int \prod_l \left(\prod_n \{d\vec{R}_n^{(l)}(t_0)\} P_0(\{\vec{R}_n^{(l)}(t_0)\})\right) \int \prod_{l,n} \left\{D[\vec{R}_n^{(l)}(t')] D[\hat{\vec{R}}_n^{(l)}(t')]\right\} \\ &\times \exp\left[\sum_{l,n}\int_{t_0}^{t} dt'\, i\hat{\vec{R}}_n^{(l)}(t')\cdot\left(\frac{\partial \vec{R}_n^{(l)}(t')}{\partial t'} - \frac{1}{\zeta_0}\vec{F}_n^{(l)}(t') - \frac{1}{\zeta_0}\vec{F}_{ext}(\vec{R}_n^{(l)}(t'))\right.\right. \\ &- \left.\left. \frac{1}{\zeta_0}\sum_{l',m}\vec{F}_{int}(\vec{R}_n^{(l)}(t'),\vec{R}_m^{(l')}(t')) + \frac{ik_BT}{\zeta_0}\hat{\vec{R}}_n^{(l)}(t')\right)\right]. \end{aligned} \tag{B.9}$$

B.2 Recursion relation for $Q([\omega,\boldsymbol{\psi}],t|t_0)$

Starting with the definition of the dynamical single-chain partition function $Q([\omega,\boldsymbol{\psi}],t|t_0)$ (Eq. 3.1) we discretize time in intervals of size Δt, where $t_K = t$:

$$\begin{aligned} Q([\omega,\boldsymbol{\psi}],t_K|t_0) &= \int \prod_n \left\{d\vec{R}_n(t_K) d\hat{\vec{R}}_n(t_K) d\vec{R}_n(t_{K-1}) d\hat{\vec{R}}_n(t_{K-1}) \ldots d\vec{R}_n(t_2)\right. \\ &\times \left. d\hat{\vec{R}}_n(t_2) d\vec{R}_n(t_1) d\hat{\vec{R}}_n(t_1) d\vec{R}_n(t_0)\right\} P_0(\{\vec{R}_n(t_0)\}) \\ &\times \prod_n \prod_{i=1}^{K} \exp\left(i\hat{\vec{R}}_n(t_i)\cdot\left\{\vec{R}_n(t_i) - \vec{R}_n(t_{i-1}) - \frac{\Delta t}{\zeta_0}\vec{F}_n(t_i) -\right.\right. \\ &- \left.\left. \Delta t\boldsymbol{\psi}(\vec{R}_n(t_i),t_i) + \frac{i\Delta t k_B T}{\zeta_0}\hat{\vec{R}}_n(t_i)\right\} - i\Delta t\omega(\vec{R}_n(t_i),t_i)\right) \end{aligned} \tag{B.10}$$

Note the lack of a $\hat{\vec{R}}_n(t_0)$ term. Since our discretization scheme is such that

$$\frac{\partial \vec{R}_n(t)}{\partial t} \Rightarrow \frac{\vec{R}_n(t_i) - \vec{R}_n(t_{i-1})}{\Delta t} \tag{B.11}$$

we choose to enforce the Langevin equation only for $t > t_0$ since we already know the state of the system at t_0: that is, it is given by the probability distribution $P_0(\{\vec{R}_n(t_0)\})$. Given this discretized form of $Q([\omega, \boldsymbol{\psi}], t_K|t_0)$, the integral can be formulated iteratively by defining the quantity $q(\{\vec{R}_n(t_i)\}, t_i|t_0)$ and the following recursion relations:

$$\begin{aligned} q(\{\vec{R}_n(t_1)\}, t_1|t_0) &= \exp\left(-i\sum_n \Delta t\omega(\vec{R}_n(t_1), t_1)\right) \int \prod_n \left\{d\hat{\vec{R}}_n(t_1) d\vec{R}_n(t_0)\right\} \\ &\times \exp\left\{i\sum_n \hat{\vec{R}}_n(t_1) \cdot \left(\vec{R}_n(t_1) - \vec{R}_n(t_0) - \frac{\Delta t}{\zeta_0}\vec{F}_n(t_1)\right.\right. \\ &- \left.\left. \Delta t\boldsymbol{\psi}(\vec{R}_n(t_1), t_1) + i\frac{\Delta t k_B T}{\zeta_0}\hat{\vec{R}}_n(t_1)\right)\right\} P(\{\vec{R}_n(t_0)\}), \quad \text{(B.12)} \end{aligned}$$

$$\begin{aligned} q(\{\vec{R}_n(t_2)\}, t_2|t_0) &= \exp\left(-i\sum_n \Delta t\omega(\vec{R}_n(t_2), t_2)\right) \int \prod_n \left\{d\hat{\vec{R}}_n(t_2) d\vec{R}_n(t_1)\right\} \\ &\times \exp\left\{i\sum_n \hat{\vec{R}}_n(t_2) \cdot \left(\vec{R}_n(t_2) - \vec{R}_n(t_1) - \frac{\Delta t}{\zeta_0}\vec{F}_n(t_2)\right.\right. \\ &- \left.\left. \Delta t\boldsymbol{\psi}(\vec{R}_n(t_2), t_2) + i\frac{\Delta t k_B T}{\zeta_0}\hat{\vec{R}}_n(t_2)\right)\right\} \\ &\times q(\{\vec{R}_n(t_1)\}, t_1|t_0) \quad \text{(B.13)} \end{aligned}$$

and so on for all t_i. The general recursion relation is given by

$$\begin{aligned} q(\{\vec{R}_n(t_{i+1})\}, t_{i+1}|t_0) &= \exp\left(-i\sum_n \Delta t\omega(\vec{R}_n(t_{i+1}), t_{i+1})\right) \int \prod_n \left\{d\hat{\vec{R}}_n(t_{i+1}) d\vec{R}_n(t_i)\right\} \\ &\times \exp\left\{i\sum_n \hat{\vec{R}}_n(t_{i+1}) \cdot \left(\vec{R}_n(t_{i+1}) - \vec{R}_n(t_i) - \frac{\Delta t}{\zeta_0}\vec{F}_n(t_{i+1})\right.\right. \\ &- \left.\left. \Delta t\boldsymbol{\psi}(\vec{R}_n(t_{i+1}), t_{i+1}) + i\frac{\Delta t k_B T}{\zeta_0}\hat{\vec{R}}_n(t_{i+1})\right)\right\} \\ &\times q(\{\vec{R}_n(t_i)\}, t_i|t_0). \quad \text{(B.14)} \end{aligned}$$

We may define $q(\{\vec{r}_n\}, t_i|t_0)$, where we have relabeled $\vec{R}_n(t_i)$ as $\vec{r}_n$ for convenience. This replacement is unambiguous because the context in which it is used (as an argument of $q(\{\vec{r}_n\}, t_i|t_0)$) makes it clear that $\vec{r}_n$ is defined at time t_i. Eq. B.14 becomes

$$\begin{aligned} q(\{\vec{r}_n\}, t_{i+1}|t_0) &= \exp\left(-\sum_n \Delta t i\omega(\vec{r}_n, t_{i+1})\right) \int \prod_n \left\{d\hat{\vec{r}}_n d\vec{r}'_n\right\} \\ &\times \exp\left\{\sum_n i\hat{\vec{r}}_n \cdot \left(\vec{r}_n - \vec{r}'_n - \frac{\Delta t}{\zeta_0}\vec{F}_n(t_{i+1})\right.\right. \\ &- \left.\left. \Delta t\boldsymbol{\psi}(\vec{r}_n, t_{i+1}) + \frac{i\Delta t k_B T}{\zeta_0}\hat{\vec{r}}_n\right)\right\} q(\{\vec{r}'_n\}, t_i|t_0). \end{aligned} \tag{B.15}$$

This is Equation 3.4. Note also the connection to $Q([\omega, \boldsymbol{\psi}], t_K|t_0)$:

$$Q([\omega, \boldsymbol{\psi}], t_K|t_0) = \int \{d\vec{r}_n\} q(\{\vec{r}_n\}, t_K|t_0). \tag{B.16}$$

B.3 Modified Fokker-Planck equation

The modified Fokker-Planck equation may be derived from Eq. B.15. First, terms in Eq. B.15 are expanded to first order in Δt:

$$\begin{aligned} q(\{\vec{r}_n\}, t_{i+1}|t_0) &= \left(1 - i\sum_n \Delta t\omega(\vec{r}_n, t_{i+1})\right) \int \prod_n \left\{d\hat{\vec{r}}_n d\vec{r}'_n\right\} \\ &\times \exp\left\{i\sum_n \hat{\vec{r}}_n \cdot (\vec{r}_n - \vec{r}'_n)\right\} \left(1 - \frac{\Delta t}{\zeta_0}\sum_n i\hat{\vec{r}}_n \cdot \vec{F}_n(t_{i+1})\right. \\ &- \left. i\Delta t\sum_n \hat{\vec{r}}_n \cdot \boldsymbol{\psi}(\vec{r}_n, t_{i+1}) - \frac{\Delta t k_B T}{\zeta_0}\sum_n \hat{r}_n^2\right) q(\{\vec{r}'_n\} t_i|t_0). \end{aligned} \tag{B.17}$$

Noting that

$$\int \prod_n \left\{d\hat{\vec{r}}_n\right\} \exp\{i\hat{\vec{r}}_n \cdot (\vec{r}_n - \vec{r}'_n)\} = \prod_n \delta(\vec{r}_n - \vec{r}'_n) \tag{B.18}$$

and

$$\begin{aligned}
&\int \prod_n \{d\hat{\vec{r}}_n\} i\hat{\vec{r}}_m \exp\left\{ i \sum_n \hat{\vec{r}}_n \cdot (\vec{r}_n - \vec{r}'_n) \right\} \\
&= -\int \prod_n \{d\hat{\vec{r}}_n\} \nabla_{\vec{r}'_m} \exp\left\{ i \sum_n \hat{\vec{r}}_n \cdot (\vec{r}_n - \vec{r}'_n) \right\} \\
&= -\nabla_{\vec{r}'_m} \prod_n \delta(\vec{r}_n - \vec{r}'_n) \qquad \text{(B.19)}
\end{aligned}$$

where $\nabla_{\vec{r}'_m}$ is a gradient of $\vec{r}'_m = (x'_m, y'_m, z'_m)$; that is, in three dimensions

$$\nabla_{\vec{r}'_m} = \left(\frac{\partial}{\partial x'_m}, \frac{\partial}{\partial y'_m}, \frac{\partial}{\partial z'_m} \right), \qquad \text{(B.20)}$$

we can rewrite the recursion relation in the form

$$\begin{aligned}
q(\{\vec{r}_n\}, t_{i+1}|t_0) &= \left(1 - i \sum_n \Delta t \omega(\vec{r}_n, t_{i+1}) \right) \int \prod_n \{d\vec{r}'_n\} \\
&\times \; q(\{\vec{r}'_n\}, t_i|t_0) \left(1 + \frac{\Delta t}{\zeta_0} \sum_n \vec{F}_n(t_{i+1}) \cdot \nabla_{\vec{r}'_n} \right. \\
&+ \left. \sum_n \Delta t \boldsymbol{\psi}(\vec{r}_n, t_{i+1}) \cdot \nabla_{\vec{r}'_n} + \frac{\Delta t k_B T}{\zeta_0} \sum_n \nabla^2_{\vec{r}'_n} \right) \\
&\times \; \prod_n \delta(\vec{r}_n - \vec{r}'_n) \qquad \text{(B.21)}
\end{aligned}$$

We need consider only terms that are of $\mathcal{O}(\Delta t)$ (for reasons that will become apparent below). Since $\vec{r}_n$ and $\vec{r}'_n$ are defined at t_{i+1} and t_i, respectively, we may Taylor-series expand ($t_{i+1} \to t_i + \mathcal{O}(\Delta t)$) functions of $\vec{r}_n$ and by keeping only terms of $\mathcal{O}(\Delta t)$, we simply replace $\omega(\vec{r}_n, t_{i+1})$, $\vec{F}_n(t_{i+1})$ and $\boldsymbol{\psi}(\vec{r}_n, t_{i+1})$ with $\omega(\vec{r}_n, t_i)$, $\vec{F}_n(t_i)$ and $\boldsymbol{\psi}(\vec{r}_n, t_i)$,

respectively. Integration by parts of the integrals over $\vec{r}'_n$ gives

$$\begin{aligned} q(\{\vec{r}_n\}, t_{i+1}|t_0) &= \left(1 - i\sum_n \Delta t \omega(\vec{r}_n, t_i)\right) \int \prod_n \{d\vec{r}'_n \delta(\vec{r}_n - \vec{r}'_n)\} \\ &\times \left(q(\{\vec{r}'_n\}, t_i|t_0) - \Delta t \sum_n \left\{\nabla_{\vec{r}'_n} \cdot \left(\frac{1}{\zeta_0}\vec{F}_n(t_i) q(\{\vec{r}'_n\}, t_i|t_0)\right)\right.\right. \\ &+ \nabla_{\vec{r}'_n} \cdot (\boldsymbol{\psi}(\vec{r}'_n, t_i) q(\{\vec{r}'_n\}, t_i|t_0)) \\ &- \left.\left. \frac{k_B T}{\zeta_0} \nabla^2_{\vec{r}'_n} q(\{\vec{r}'_n\}, t_i|t_0)\right\}\right). \end{aligned} \tag{B.22}$$

The integrals can be easily evaluated using the properties of the delta function:

$$\begin{aligned} q(\{\vec{r}_n\}, t_{i+1}|t_0) &= q(\{\vec{r}_n\}, t_i|t_0) + \frac{\Delta t k_B T}{\zeta_0} \sum_n \nabla^2_{\vec{r}_n} q(\{\vec{r}_n\}, t_i|t_0) \\ &- \Delta t \sum_n \nabla_{\vec{r}_n} \cdot \left\{\left(\frac{1}{\zeta_0}\vec{F}_n(t_i) + \boldsymbol{\psi}(\vec{r}_n, t_i)\right) q(\{\vec{r}_n\}, t_i|t_0)\right\} \\ &- i\Delta t \sum_n \omega(\vec{r}_n, t_i) q(\{\vec{r}_n\}, t_i|t_0) \end{aligned} \tag{B.23}$$

Dividing Eq. B.23 by Δt and rearranging, we have

$$\begin{aligned} \frac{q(\{\vec{r}_n\}, t_{i+1}|t_0) - q(\{\vec{r}_n\}, t_i|t_0)}{\Delta t} &= \frac{k_B T}{\zeta_0} \sum_n \nabla^2_{\vec{r}_n} q(\{\vec{r}_n\}, t_i|t_0) \\ &- \sum_n \nabla_{\vec{r}_n} \cdot \left(\frac{1}{\zeta_0}\vec{F}_n(t_i) q(\{\vec{r}_n\}, t_i|t_0)\right) \\ &- \sum_n \nabla_{\vec{r}_n} \cdot (\boldsymbol{\psi}(\vec{r}_n, t_i) q(\{\vec{r}_n\}, t_i|t_0)) \\ &- i\sum_n \omega(\vec{r}_n, t_i) q(\{\vec{r}_n\}, t_i|t_0). \end{aligned} \tag{B.24}$$

Taking the limits as $\Delta t \to 0$ and $t_i \to t$, we apply the definition of the partial derivative with respect to t and arrive at the modified Fokker-Planck equation, Eq. 3.5

$$\begin{aligned}\frac{\partial q(\{\vec{r}_n\},t|t_0)}{\partial t} &= \frac{k_B T}{\zeta_0}\sum_n \nabla^2_{\vec{r}_n} q(\{\vec{r}_n\},t|t_0) \\ &- \sum_n \nabla_{\vec{r}_n}\cdot\left(\frac{1}{\zeta_0}\vec{F}_n(t)q(\{\vec{r}_n\},t|t_0)\right) \\ &- \sum_n \nabla_{\vec{r}_n}\cdot(\boldsymbol{\psi}(\vec{r}_n,t)q(\{\vec{r}_n\},t|t_0)) \\ &- i\left[\sum_n \omega(\vec{r}_n,t)\right] q(\{\vec{r}_n\},t|t_0). \end{aligned} \tag{B.25}$$

B.4 Multiplicative property of $q(\{\vec{r}_n\},t|t_0)$

We would expect $q(\{\vec{r}_n\},t|t_0)$ to possess the multiplicative property that would be associated with a conditional probability distribution. By inserting

$$1 = \int \prod_n \{d\vec{r}'_n\}\delta(\vec{r}'_n - \vec{R}_n(t_m)) \tag{B.26}$$

into Eq. B.10, where $t_K > t_m > t_0$, the recursion proceeds as before up to the integral over $\vec{R}_n(t_m)$:

$$\begin{aligned} Q([\omega,\boldsymbol{\psi}],t|t_0) &= \int\prod_n\{d\vec{r}'_n\}\int\prod_n\{d\vec{R}_n(t_K)d\hat{\vec{R}}_n(t_K)d\vec{R}_n(t_{K-1})d\hat{\vec{R}}_n(t_{K-1})\cdots \\ &\times\ d\vec{R}_n(t_{m+1})d\hat{\vec{R}}_n(t_{m+1})d\vec{R}_n(t_m)\}\prod_{i=m}^{K-1}\exp\left(i\sum_n \hat{\vec{R}}_n(t_{i+1})\right. \\ &\cdot\ \left\{\vec{R}_n(t_{i+1}) - \vec{R}_n(t_i) - \frac{\Delta t}{\zeta_0}\vec{F}_n(t_{i+1}) - \Delta t\boldsymbol{\psi}(\vec{R}_n(t_{i+1}),t_{i+1})\right. \\ &+\ \left.\left. i\frac{\Delta t k_B T}{\zeta_0}\hat{\vec{R}}_n(t_{i+1})\right\} - i\Delta t\omega(\vec{R}_n(t_{i+1}),t_{i+1})\right) \\ &\times\ \prod_n \delta(\vec{r}'_n - \vec{R}_n(t_m))q(\{\vec{R}_n(t_m)\},t_m|t_0). \end{aligned} \tag{B.27}$$

Due to the properties of the delta function, $q(\{\vec{R}_n(t_m)\}, t_m|t_0)$ can be extracted from the integral. We define

$$\begin{aligned} q(\{\vec{R}_n(t_K)\}, t_K|\{\vec{r}'_n\}, t_m) &= \int \prod_n \{d\hat{\vec{R}}_n(t_K) d\vec{R}_n(t_{K-1}) \cdots d\hat{\vec{R}}_n(t_{m+1}) d\vec{R}_n(t_m)\} \\ &\times \prod_{i=m}^{K-1} \exp\left(i \sum_n \hat{\vec{R}}_n(t_{i+1}) \cdot \left\{ \vec{R}_n(t_{i+1}) - \vec{R}_n(t_i) \right.\right. \\ &- \frac{\Delta t}{\zeta_0} \vec{F}_n(t_{i+1}) - \Delta t \boldsymbol{\psi}(\vec{R}_n(t_{i+1}), t_{i+1}) \\ &+ \left.\left. i \frac{\Delta t k_B T}{\zeta_0} \hat{\vec{R}}_n(t_{i+1}) \right\} - \Delta t \omega(\vec{R}_n(t_{i+1}), t_{i+1}) \right) \\ &\times \prod_n \delta(\vec{r}'_n - \vec{R}_n(t_m)) \end{aligned} \tag{B.28}$$

which is proportional to the probability that the chain has the conformation $\{\vec{R}_n(t_K)\}$ at time t_K if it had the conformation $\{\vec{r}'_n\}$ at time t_m. $Q([\omega, \boldsymbol{\psi}], t|t_0)$ can now be written in the form

$$\begin{aligned} Q([\omega, \boldsymbol{\psi}], t|t_0) &= \int \prod_n \{d\vec{r}'_n\} \int \prod_n \{d\vec{r}_n\} q(\{\vec{r}_n\}, t|\{\vec{r}'_n\}, t') \\ &\times q(\{\vec{r}'_n\}, t'|t_0), \end{aligned} \tag{B.29}$$

where we have replaced t_m with t'. By comparison with Eq. 3.2, we may write

$$q(\{\vec{r}_n\}, t|t_0) = \int \prod_n \{d\vec{r}'_n\} q(\{\vec{r}_n\}, t|\{\vec{r}'_n\}, t') q(\{\vec{r}'_n\}, t'|t_0), \tag{B.30}$$

which is the multiplicative property we seek.

B.5 Functional derivatives of $Q([\omega, \boldsymbol{\psi}], t|t_0)$

Functional derivatives of $Q([\omega, \boldsymbol{\psi}], t|t_0)$ with respect to ω generate density correlation functions. Using Eq. 3.1 and the standard definition of the functional derivative:

$$\begin{aligned}
\frac{\delta Q[\omega(\vec{R}_n(t'), t'), \boldsymbol{\psi}], t|t_0}{\delta\omega(\vec{r}, t)} &= \lim_{\epsilon\to 0}\frac{1}{\epsilon}\Big(Q([\omega + \epsilon\delta(t'-t)\delta(\vec{r}-\vec{R}_n(t')), \boldsymbol{\psi}], t|t_0) - Q([\omega, \boldsymbol{\psi}], t|t_0)\Big) \\
&= \lim_{\epsilon\to 0}\frac{1}{\epsilon}\int\prod_n\{d\vec{R}_n(t_0)\}P_0(\{\vec{R}_n(t_0)\})\int\prod_n\Big\{D[\vec{R}_n(t')] \\
&\times \quad D[\hat{\vec{R}}_n(t')]\Big\}\left[\exp\left\{\sum_n\int_{t_0}^{t}dt'\, i\hat{\vec{R}}_n(t')\cdot\left(\frac{\partial\vec{R}_n(t')}{\partial t'} - \frac{1}{\zeta_0}\vec{F}_n(t')\right.\right.\right. \\
&- \quad \left.\left.\left.\boldsymbol{\psi}(\vec{R}_n(t'), t') + \frac{ik_BT}{\zeta_0}\hat{\vec{R}}_n(t')\right)\right\} \\
&\times \quad \left(\exp\left\{-\sum_n\int_{t_0}^{t}dt'\, i\left[\omega(\vec{R}_n(t'), t') + \epsilon\delta(t'-t)\delta(\vec{r}-\vec{R}_n(t'))\right]\right\}\right. \\
&- \quad \left.\exp\left\{-\sum_n\int_{t_0}^{t}dt'\, i\omega(\vec{R}_n(t'), t')\right\}\right)\Bigg]. \qquad \text{(B.31)}
\end{aligned}$$

The $\exp\left(-i\epsilon\sum_n\int_{t_0}^{t}dt'\,\delta(t'-t)\delta(\vec{r}-\vec{R}_n(t'))\right)$ term may be expanded up to $\mathcal{O}(\epsilon)$:

$$\begin{aligned}
\exp\left(-i\epsilon\sum_n\int_{t_0}^{t}dt'\,\delta(t'-t)\delta(\vec{r}-\vec{R}_n(t'))\right) &\approx 1 - i\epsilon\sum_n\lim_{t''\to t^+}\int_{t_0}^{t''}dt'\,\delta(t'-t'') \\
&\times \quad \delta(\vec{r}-\vec{R}_n(t')) \\
&\approx 1 - i\epsilon\sum_n\delta(\vec{r}-\vec{R}_n(t)). \qquad \text{(B.32)}
\end{aligned}$$

The functional derivative is then given by

$$\begin{aligned}\frac{\delta Q([\omega,\boldsymbol{\psi}],t|t_0)}{\delta\omega(\vec{r},t)} &= \lim_{\epsilon\to 0}\frac{1}{\epsilon}\Bigg[Q([\omega,\boldsymbol{\psi}],t|t_0) - i\epsilon\int\prod_n\left\{d\vec{R}_n(t_0)P_0(\{\vec{R}_n(t_0)\})\right\}\\ &\times \int\prod_n\left\{D[\vec{R}_n(t')]D[\hat{\vec{R}}_n(t')]\right\}\sum_n\delta(\vec{r}-\vec{R}_n(t))\\ &\times \exp\left(\sum_n\int_{t_0}^{t}dt'\,i\hat{\vec{R}}_n(t')\cdot\left(\frac{\partial\vec{R}_n(t')}{\partial t'}-\frac{1}{\zeta_0}\vec{F}_n(t')-\boldsymbol{\psi}(\vec{R}_n(t'),t')\right.\right.\\ &+ \left.\left.\frac{ik_BT}{\zeta_0}\hat{\vec{R}}_n(t')\right)-\sum_n\int_{t_0}^{t}dt'\,i\omega(\vec{R}_n(t'),t')\right)-Q([\omega,\boldsymbol{\psi}],t|t_0)\Bigg].\end{aligned} \tag{B.33}$$

Cancelling $Q([\omega,\boldsymbol{\psi}],t|t_0)$s and the factors of ϵ, we have

$$\begin{aligned}\frac{\delta Q([\omega,\boldsymbol{\psi}],t|t_0)}{\delta\omega(\vec{r},t)} &= -iQ([\omega,\boldsymbol{\psi}],t|t_0)\left\langle\sum_n\delta(\vec{r}-\vec{R}_n(t))\right\rangle\\ &= -iQ([\omega,\boldsymbol{\psi}])\left\langle\hat{\rho}_0(\vec{r},t)\right\rangle\end{aligned} \tag{B.34}$$

where $\hat{\rho}_0(\vec{r},t)$ is the single-chain density field, and $Q([\omega,\boldsymbol{\psi}],t|t_0)$ appears since it is the normalization constant for averages. This also serves as an alternate derivation of the functional derivative calculated in Section 3.3, since

$$\sum_n\left\langle\delta(\vec{r}-\vec{R}_n(t))\right\rangle=\sum_n\frac{q(\vec{r},n,t|t_0)}{Q([\omega,\boldsymbol{\psi}],t|t_0)}. \tag{B.35}$$

An extension of the derivation done here shows that second functional derivatives of $Q([\omega,\boldsymbol{\psi}],t|t_0)$ with respect to ω generate density correlation functions. The second derivative brings down a second factor of ρ:

$$\begin{aligned}\frac{\delta^2 Q([\omega,\boldsymbol{\psi}],t|t_0)}{\delta\omega(\vec{r},t)\delta\omega(\vec{r}',t'')} &= -Q([\omega,\boldsymbol{\psi}],t|t_0)\left\langle\sum_{n,m}\delta(\vec{r}-\vec{R}_n(t))\delta(\vec{r}'-\vec{R}_m(t''))\right\rangle\\ &= -Q([\omega,\boldsymbol{\psi}],t|t_0)\left\langle\hat{\rho}_0(\vec{r},t)\hat{\rho}_0(\vec{r}',t'')\right\rangle\end{aligned} \tag{B.36}$$

where $t \geq t'' \geq t_0$. If $t'' > t$, it is the latest time appearing in the average and $Q([\omega, \boldsymbol{\psi}], t|t_0)$ is then $Q([\omega, \boldsymbol{\psi}], t''|t_0)$; that is, the time argument of $Q([\omega, \boldsymbol{\psi}], t|t_0)$ is always the latest time appearing in the average.

B.6 Generalization of the formalism to a binary system

We may extend the formalism to consider a binary system consisting of n_A polymers of type A and n_B polymers of type B, with degrees of polymerization N_A and N_B, respectively. The Langevin equation must be enforced for both species of polymer

$$\begin{aligned} \zeta_0 \frac{\partial \vec{R}_n^{(a)}(t)}{\partial t} &= \vec{F}_n^{(a)}(t) + \vec{F}_{ext}^{A}(\vec{R}_n^{(a)}(t)) + \sum_{a'} \sum_m \vec{F}_{int}^{AA}(\vec{R}_n^{(a)}(t), \vec{R}_m^{(a')}(t)) \\ &+ \sum_b \sum_m \vec{F}_{int}^{AB}(\vec{R}_n^{(a)}(t), \vec{R}_m^{(b)}(t)) + \vec{f}_n^{(a)}(t) \end{aligned} \tag{B.37}$$

and

$$\begin{aligned} \zeta_0 \frac{\partial \vec{R}_n^{(b)}(t)}{\partial t} &= \vec{F}_n^{(b)}(t) + \vec{F}_{ext}^{B}(\vec{R}_n^{(b)}(t)) + \sum_{b'} \sum_m \vec{F}_{int}^{BB}(\vec{R}_n^{(b)}(t), \vec{R}_m^{(b')}(t)) \\ &+ \sum_a \sum_m \vec{F}_{int}^{AB}(\vec{R}_n^{(b)}(t), \vec{R}_m^{(a)}(t)) + \vec{f}_n^{(b)}(t), \end{aligned} \tag{B.38}$$

where we label the polymers of type A with a and type B with b, and we have introduced the interaction forces $\vec{F}_{int}^{AA}$, $\vec{F}_{int}^{BB}$ and $\vec{F}_{int}^{AB}$ as the forces between like and unlike polymer types. We construct the functional integral and perform the noise

average:

$$
\begin{aligned}
Z(t|t_0) &= \int \prod_{a,b} \left(\prod_n \{ d\vec{R}_n^{(a)}(t_0) d\vec{R}_n^{(b)}(t_0) \} P_0(\{\vec{R}_n^{(a)}(t_0) P_0(\{\vec{R}_n^{(b)}(t_0)\}) \right) \\
&\times \int \prod_{a,n,b} \left\{ D[\vec{R}_n^{(a)}(t')] D[\hat{\vec{R}}_n^{(a)}(t')] D[\vec{R}_n^{(b)}(t')] D[\hat{\vec{R}}_n^{(b)}(t')] \right\} \\
&\times \exp\left[\sum_{a,n} \int_{t_0}^{t} dt'\, i\hat{\vec{R}}_n^{(a)}(t') \cdot \left(\frac{\partial \vec{R}_n^{(a)}(t')}{\partial t'} - \frac{1}{\zeta_0} \vec{F}_n^{(a)}(t') - \frac{1}{\zeta_0} \vec{F}_{ext}^{A}(\vec{R}_n^{(a)}(t')) \right.\right. \\
&- \frac{1}{\zeta_0} \sum_{a',m} \vec{F}_{int}^{AA}(\vec{R}_n^{(a)}(t'), \vec{R}_m^{(a')}(t')) - \frac{1}{\zeta_0} \sum_{b,m} \vec{F}_{int}^{AB}(\vec{R}_n^{(a)}(t'), \vec{R}_m^{(b)}(t')) \\
&+ \left.\left. \frac{ik_B T}{\zeta_0} \hat{\vec{R}}_n^{(a)}(t') \right) \right] \\
&\times \exp\left[\sum_{b,n} \int_{t_0}^{t} dt'\, i\hat{\vec{R}}_n^{(b)}(t') \cdot \left(\frac{\partial \vec{R}_n^{(b)}(t')}{\partial t'} - \frac{1}{\zeta_0} \vec{F}_n^{(b)}(t') - \frac{1}{\zeta_0} \vec{F}_{ext}^{B}(\vec{R}_n^{(b)}(t')) \right.\right. \\
&- \frac{1}{\zeta_0} \sum_{b',m} \vec{F}_{int}^{BB}(\vec{R}_n^{(b)}(t'), \vec{R}_m^{(b')}(t')) - \frac{1}{\zeta_0} \sum_{a,m} \vec{F}_{int}^{AB}(\vec{R}_n^{(b)}(t'), \vec{R}_m^{(a)}(t')) \\
&+ \left.\left. \frac{ik_B T}{\zeta_0} \hat{\vec{R}}_n^{(b)}(t') \right) \right]. \qquad \text{(B.39)}
\end{aligned}
$$

The collective field variables are

$$
\begin{aligned}
\hat{\rho}_A(\vec{r}, t) &= \sum_{a,n} \delta(\vec{r} - \vec{R}_n^{(a)}(t)) \qquad \text{(B.40)} \\
\hat{\rho}_B(\vec{r}, t) &= \sum_{b,n} \delta(\vec{r} - \vec{R}_n^{(b)}(t)) \qquad \text{(B.41)} \\
\hat{\boldsymbol{\phi}}_A(\vec{r}, t) &= \sum_{a,n} \hat{\vec{R}}_n^{(a)}(t) \delta(\vec{r} - \vec{R}_n^{(a)}(t)) \qquad \text{(B.42)} \\
\hat{\boldsymbol{\phi}}_B(\vec{r}, t) &= \sum_{b,n} \hat{\vec{R}}_n^{(b)}(t) \delta(\vec{r} - \vec{R}_n^{(b)}(t)). \qquad \text{(B.43)}
\end{aligned}
$$

We follow the same procedure as in Section 2.3, and, by introducing the fields ρ_A, ρ_B, $\boldsymbol{\phi}_A$, $\boldsymbol{\phi}_B$, ω_A, ω_B, $\boldsymbol{\psi}_A$ and $\boldsymbol{\psi}_B$, write $Z(t|t_0)$ as

$$\begin{aligned} Z(t|t_0) &= \int D[\rho_A]D[\rho_B]D[\omega_A]D[\omega_B]D[\boldsymbol{\phi}_A]D[\boldsymbol{\phi}_B]D[\boldsymbol{\psi}_A]D[\boldsymbol{\psi}_B] \\ &\times \exp\left(-L[\rho_A,\rho_B,\omega_A,\omega_B,\boldsymbol{\phi}_A,\boldsymbol{\phi}_B,\boldsymbol{\psi}_A,\boldsymbol{\psi}_B]\right) \end{aligned} \tag{B.44}$$

where the effective action L takes the form

$$\begin{aligned} L[\rho_{A,B},\omega_{A,B},\boldsymbol{\phi}_{A,B},\boldsymbol{\psi}_{A,B}] &= -i\int d\vec{r}\int_{t_0}^{t} dt' \ (\boldsymbol{\phi}_A(\vec{r},t')\cdot\boldsymbol{\psi}_A(\vec{r},t') + \boldsymbol{\phi}_B(\vec{r},t')\cdot\boldsymbol{\psi}_B(\vec{r},t') \\ &+ \omega_A(\vec{r},t')\rho_A(\vec{r},t') + \omega_B(\vec{r},t')\rho_B(\vec{r},t')) \\ &+ \frac{i}{\zeta_0}\int d\vec{r}\int_{t_0}^{t} dt' \ \Big[\boldsymbol{\phi}_A(\vec{r},t')\cdot\vec{F}^{A}_{ext}(\vec{r}) + \boldsymbol{\phi}_B(\vec{r},t')\cdot\vec{F}^{B}_{ext}(\vec{r}) \\ &+ \int d\vec{r}' \Big(\rho_A(\vec{r}',t')\boldsymbol{\phi}_A(\vec{r},t')\cdot\vec{F}^{AA}_{int}(\vec{r},\vec{r}') \\ &+ \rho_B(\vec{r}',t')\boldsymbol{\phi}_B(\vec{r},t')\cdot\vec{F}^{BB}_{int}(\vec{r},\vec{r}') + \rho_B(\vec{r}',t')\boldsymbol{\phi}_A(\vec{r},t')\cdot\vec{F}^{AB}_{int}(\vec{r},\vec{r}') \\ &+ \rho_A(\vec{r}',t')\boldsymbol{\phi}_B(\vec{r},t')\cdot\vec{F}^{AB}_{int}(\vec{r},\vec{r}')\Big)\Big] \\ &- n_A \ln Q_A([\omega_A,\boldsymbol{\psi}_A],t|t_0) - n_B \ln Q_B([\omega_B,\boldsymbol{\psi}_B],t|t_0) \end{aligned} \tag{B.45}$$

and $Q_A([\omega_A,\boldsymbol{\psi}_A],t|t_0)$ and $Q_B([\omega_B,\boldsymbol{\psi}_B],t|t_0)$ are

$$\begin{aligned} Q_A([\omega_A,\boldsymbol{\psi}_A],t|t_0) &= \int\prod_n\{d\vec{R}_n(t_0)\}P_0(\{\vec{R}_n(t_0)\})\int\prod_n\Big\{D[\vec{R}_n(t')]D[\hat{\vec{R}}_n(t')]\Big\} \\ &\times \exp\left(\sum_n\int_{t_0}^{t} dt'\, i\hat{\vec{R}}_n(t')\cdot\left(\frac{\partial\vec{R}_n(t')}{\partial t'} - \frac{1}{\zeta_0}\vec{F}_n(t') - \boldsymbol{\psi}_A(\vec{R}_n(t'),t')\right.\right. \\ &+ \left.\left.\frac{ik_BT}{\zeta_0}\hat{\vec{R}}_n(t')\right) - \sum_n\int_{t_0}^{t} dt'\, i\omega_A(\vec{R}_n(t'),t')\right) \end{aligned} \tag{B.46}$$

and

$$
\begin{aligned}
Q_B([\omega_B, \boldsymbol{\psi}_B], t|t_0) &= \int \prod_n \{d\vec{R}_n(t_0)\} P_0(\{\vec{R}_n(t_0)\}) \int \prod_n \left\{ D[\vec{R}_n(t')] D[\hat{\vec{R}}_n(t')] \right\} \\
&\times \exp\left(\sum_n \int_{t_0}^{t} dt'\, i\hat{\vec{R}}_n(t') \cdot \left(\frac{\partial \vec{R}_n(t')}{\partial t'} - \frac{1}{\zeta_0} \vec{F}_n(t') - \boldsymbol{\psi}_B(\vec{R}_n(t'), t') \right.\right. \\
&+ \left.\left. \frac{ik_B T}{\zeta_0} \hat{\vec{R}}_n(t') \right) - \sum_n \int_{t_0}^{t} dt'\, i\omega_B(\vec{R}_n(t'), t') \right). \qquad \text{(B.47)}
\end{aligned}
$$

As in the single-species case, the ω and $\boldsymbol{\phi}$ fields vanish in the mean-field approximation. The mean-field equations are

$$
\begin{aligned}
\rho_A(\vec{r}, t) &= \frac{n_A}{Q_A([\boldsymbol{\psi}_A], t|t_0)} \sum_n q_A(\vec{r}, n, t|t_0) && \text{(B.48)} \\
\rho_B(\vec{r}, t) &= \frac{n_B}{Q_B([\boldsymbol{\psi}_B], t|t_0)} \sum_n q_B(\vec{r}, n, t|t_0) && \text{(B.49)} \\
\boldsymbol{\psi}_A(\vec{r}, t) &= \frac{1}{\zeta_0} \vec{F}^A_{ext}(\vec{r}) + \frac{1}{\zeta_0} \int d\vec{r}' \left(\rho_A(\vec{r}', t) \vec{F}^{AA}_{int}(\vec{r}, \vec{r}') \right. \\
&+ \left. \rho_B(\vec{r}', t) \vec{F}^{AB}_{int}(\vec{r}, \vec{r}') \right) && \text{(B.50)} \\
\boldsymbol{\psi}_B(\vec{r}, t) &= \frac{1}{\zeta_0} \vec{F}^B_{ext}(\vec{r}) + \frac{1}{\zeta_0} \int d\vec{r}' \left(\rho_B(\vec{r}', t) \vec{F}^{BB}_{int}(\vec{r}, \vec{r}') \right. \\
&+ \left. \rho_A(\vec{r}', t) \vec{F}^{AB}_{int}(\vec{r}, \vec{r}') \right) && \text{(B.51)}
\end{aligned}
$$

and the relationships between $Q_A([\boldsymbol{\psi}_A], t|t_0)$ and $q_A(\{\vec{r}_{n_A}\}, t|t_0)$ as well as $Q_B([\boldsymbol{\psi}_B], t|t_0)$ and $q_B(\{\vec{r}_{n_B}\}, t|t_0)$ are similar to before (the functional Fokker-Planck equations are identical as well, one involving $\boldsymbol{\psi}_A$ and the other involving $\boldsymbol{\psi}_B$). This completes the formalism, and the modifications for the Brownian particle ($N_A = N_B = 1$) case with short-range repulsive interactions, used in Section 4.3.3, are trivial.

Bibliography

[1] M. Doi and S. F. Edwards, *The Theory of Polymer Dynamics*, Oxford University Press, New York, 1986.

[2] M. Muthukumar, J. Chem. Phys. **111** (1999).

[3] M. Muthukumar, J. Chem. Phys. **118** (2003).

[4] A. Gopinathan and Y. W. Kim, Phys. Rev. Lett. **99** (2007).

[5] Y. Kantor and M. Kardar, Phys. Rev. E **69** (2004).

[6] A. Cacciuto and E. Luijten, Phys. Rev. Lett. **96** (2006).

[7] J. Rousseau, G. Drouin, and G. W. Slater, Phys. Rev. Lett. **79** (1997).

[8] J. J. Kasianowicz, E. Brandin, D. Branton, and D. W. Deamer, Proc. Natl. Acad. Sci. USA **93** (1996).

[9] A. Debnath, A. K. R. Paul, and K. L. Sebastian, J. Stat. Mech. **Nov.** (2010).

[10] A. Boudenne, L. Ibos, Y. Candau, and S. Thomas, *Handbook of Multiphase Polymer Systems*, Wiley, Chichester, West Sussex, UK, 2011.

[11] G. H. Fredrickson, V. Ganesan, and F. Drolet, Macromolecules **35** (2002).

[12] E. Reister, M. Muller, and K. Binder, Phys. Rev. E **64** (2001).

[13] D. M. Hall, T. Lookman, G. H. Fredrickson, and S. Banerjee, Phys. Rev. Lett. **97** (2006).

[14] B. Narayanan, V. A. Pyramitsyn, and V. Ganesan, Macromolecules **37** (2004).

[15] R. Hasegawa and M. Doi, Macromolecules **30** (1997).

[16] J. Fraaije, J. Chem. Phys. **99** (1993).

[17] T. Kawakatsu, Phys. Rev. E **56** (1997).

[18] N. Maurits and J. Fraaije, J. Chem. Phys. **107** (1997).

[19] T. Shima et al., Macromolecules **36** (2003).

[20] E. Helfand, J. Chem. Phys. **63** (1975).

[21] M. Matsen and M. Schick, Phys. Rev. Lett. **72** (1994).

[22] M. W. Matsen and F. S. Bates, Macromolecules **29** (1996).

[23] C. A. Tyler and D. C. Morse, Phys. Rev. Lett. **94** (2005).

[24] E. L. Thomas, D. M. Anderson, C. S. Henkee, and D. Hoffmann, Nature **334** (1988).

[25] R. J. Spontak, S. D. Smith, and A. Ashraf, Macromolecules **26** (1993).

[26] S. F. Edwards and K. F. Freed, J. Chem. Phys. **61** (1974).

[27] P. C. Martin, E. D. Siggia, and H. A. Rose, Phys. Rev. A **8** (1973).

[28] H. Janssen, Z. Physik B **23** (1976).

[29] C. D. Dominicis and L. Peliti, Phys. Rev. B **18** (1978).

[30] G. H. Fredrickson and E. Helfand, J. Chem. Phys. **93** (1990).

[31] V. G. Rostiashvili, M. Rehkopf, and T. A. Vilgis, J. Chem. Phys **110** (1999).

[32] S. Stepanow, J. Phys. A **17** (1984).

[33] R. V. Jensen, J. Stat. Phys. **25** (1981).

[34] Y. Nakayama and R. F. Boucher, *Introduction to Fluid Mechanics*, Butterworth-Heinemann, Oxford, 1999.

[35] Z. Ding, G. Lai, T. Sakakibara, and S. Shinohara, J. Appl. Phys. **88** (2000).

[36] M. E. J. Friese, H. Rubinsztein-Dunlop, N. R. Heckenberg, and E. W. Dearden, Appl. Opt. **35** (1996).

[37] W. H. Press, S. A. Teukolsky, W. T. Vetterling, and B. P. Flannery, *Numerical Recipes in C*, Cambridge University Press, Cambridge, 1988.